



Research Article

Two new species of *Rhipidomys* (Rodentia: Sigmodontinae) from Eastern Brazil, with comments on the taxonomy of the genus

Bruno Augusto Torres PARAHYBA CAMPOS^{1,*}, Alexandre Reis PERCEQUILLO², Gustavo MIRANDA³, Alfredo LANGGUTH⁴

¹Programa de Pós Graduação em Biodiversidade Ambiente e Saúde, Centro de Estudos Superiores de Caxias, Universidade Estadual do Maranhão

²Laboratório de Zoologia de Vertebrados, Escola Superior de Agricultura “Luiz de Queiroz”, Universidade de São Paulo

³Instituto Federal Rio Grande do Sul, Campus Rio Grande

⁴Laboratório de Mamíferos, Departamento de Sistemática e Ecologia, Universidade Federal da Paraíba

Keywords:

Eastern Brazil
Rhipidomys
Sigmodontinae
taxonomy
two new species

Article history:

Received: 14 April 2021
Accepted: 03 May 2022

Acknowledgements

We are grateful to the curators and technicians of the scientific collections visited during the present study: Mario de Vivo and Juliana Gualda (MZUSP), Pedro Cordeiro Estrela (UFPA), Leonora Costa and Yuri Leite (UFES), João Alves de Oliveira and Stella Franco (MN), Raquel Moura (UFMG), Diego Astúa (UFPE), and Roberto Portela Miguez (BMNH). Fieldwork at Parque Nacional da Serra das Confusões was conducted by a team of the Museu de Zoologia da USP, coordinated by Drs. Hussam Zaher and Miguel. T. U. Rodrigues; we like to acknowledge Ana Paula Carmignotto, Marcos Sousa, Felipe Curcio, Luis Fabio Silveira, Marcos Pêrsio Dantas Santos, Diego Astúa, Giovanna G. Montingelli, Pedro Nunes, Paulo Balduino and Andre Pessoa for support during two field seasons of sampling; we are also indebted to Deocleciano Guedes Ferreira, as head of IBAMA office in Piauí. We are also in debt with Gustavo Libardi for statistical support.

BATPC was supported by postdoctoral fellowships from CAPES. This study was financed in part by the Coordenação de Aperfeiçoamento de Pessoal de Nível Superior – Brasil (CAPES) – Finance Code 001. AL and ARP were supported by Conselho Nacional de Desenvolvimento Científico e Tecnológico (CNPq) research fellowships. ARP was also supported by Fundação de Amparo à Pesquisa de São Paulo (FAPESP).

Abstract

The cricetid rodent genus *Rhipidomys* belongs to the tribe Thomasomyini, subfamily Sigmodontinae, whose distribution covers high-and lowlands areas of South America. In a number of contributions to the taxonomy and systematics of the genus, 24 species of *Rhipidomys* were recognized by different authors until now. Here we identify 13 species of the lowland “leucodactylus” section from Brazil and named two new forms of this genus based on morphological and molecular data. One of these forms is only found at municipality of Bezerros, Pernambuco state, while the other has a more extensive distribution, being recorded in northern Goiás, west of Tocantins, southern Piauí, western portion of Bahia and northern region of Minas Gerais states. These two new species can be distinguished from the others of the genus by qualitative and quantitative characters although, like most other Brazilian species of *Rhipidomys*, they do not exhibit an autapomorphic characters. These species are diagnosed by unique combinations of character states that are operational and useful for species recognition. In general, the most valuable character sets to differentiate *Rhipidomys* species are found in the skull, external morphology being strongly variable and showing overlapping sets of characters. We compared the two new species with all Brazilian species of the “leucodactylus” section and added taxonomic comments and their phylogenetic relationships.

Introduction

The genus *Rhipidomys* Tschudi, 1845 is a member of the tribe Thomasomyini, a lineage assembling five genera and 73 species, distributed over both high-and lowlands areas of South America (Pacheco et al., 2015), it belongs to the subfamily Sigmodontinae, a diverse Neotropical cricetid radiation, with 90 genera and 450 species (Burgin et al., 2018). When compared to other members of the tribe, species of this genus are usually large sized, with tails usually longer than the head and body, reaching over 200 mm and exhibiting a distinct apical pencil or hair tuft. They also share broad hind feet with short metatarsals and long digits, with a dark patch on the dorsal side. The mystacial vibrissae are dense and very long, extending well beyond the ears. All these traits are related to the arboreal/scansorial habit exhibited by these forest specialist species (Tribe, 2015).

As a consequence of a series of contributions to the taxonomy and systematics of the genus, 24 species are currently recognized (Brito et al., 2017; Tribe, 2015; Pacheco et al., 2015; Costa et al., 2011; De la Sancha et al., 2011; Rocha et al., 2011; Tribe, 2005; Allen, 1916). The last four described species of the genus (Brito et al., 2017; Costa et al., 2011; Rocha et al., 2011) were based on newly collected specimens and

on the vast amount of new molecular data from the eastern Brazilian forms (Tribe, 2015) that allowed a new perspective on the systematics of *Rhipidomys*. Nevertheless an extra effort is in need to be done in molecular approach since several localities important from nomenclatural and biogeographic point of view lack molecular samples Tribe (2015). This is especially important for moist forest enclaves distributed over Caatinga and Cerrado.

According to Tribe (2015), species of *Rhipidomys* are arranged in three sections: the highland “fulviventor” section, the tepui (inselberg) “macconnelli” section, and the lowland “leucodactylus” section, the most widespread. In this paper we are mainly concerned with the diversity of the Brazilian lowland “leucodactylus” section of the genus, stimulated by recent collecting efforts in poorly known areas of north-eastern Brazil.

Specimens from Pernambuco, Piauí, Bahia and Minas Gerais, housed in several Brazilian institutions, revealed that they represent two unique lineages with exclusive morphologic traits that lie outside the limits of hitherto known species of the genus as defined in the current literature (Tribe, 2015; Costa et al., 2011; Rocha et al., 2011; Tribe, 2005). To test these species hypothesis we conducted an integrative analysis with morphometrics and multivariate approaches, phylogenetic reconstruction and molecular species delimitation analysis. Therefore, in this contribution we aim to describe these two new species of

*Corresponding author

Email address: atpcampos@gmail.com (Bruno Augusto Torres PARAHYBA CAMPOS)

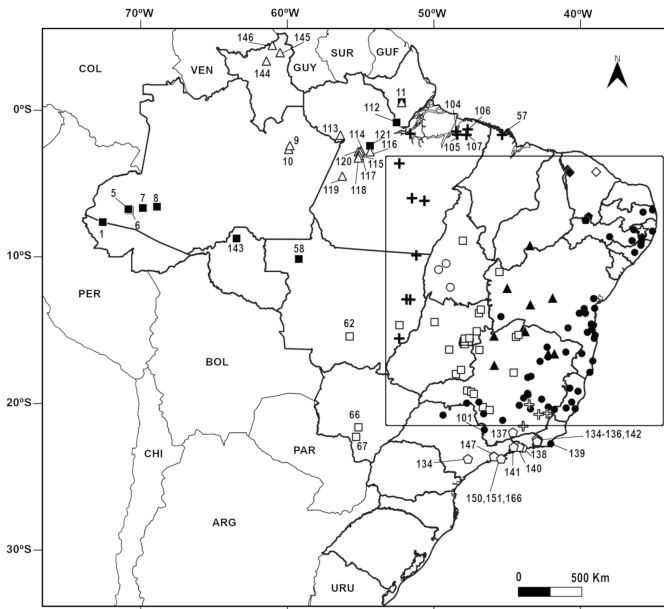


Figure 1 – Collecting localities of 13 species of the *Rhipidomys* “leucodactylus” section in Brazil. The area delimited by a square is enlarged in Fig. 2. A list of localities with the numbers shown in the maps is given in the gazetteer (Appendix C). ARG=Argentina, BOL=Bolivia, CHI=Chile, COL=Colombia, GUF=French Guiana, GUY=Guiana, PAR=Paraguay, PER=Peru, SUR=Suriname, URU=Uruguay, VEN=Venezuela. Species symbols are: ◆ *R. cariri*, ◇ *R. baturiteensis*, ☆ Specimens from Bezerros, Pernambuco, △ *R. nitela*, ○ *R. ipukensis*, ⊕ *R. tribei*, □ *R. macrurus*, ● *R. mastacalis*, ■ *R. leucodactylus*, ○ *R. itoan*, ⊕ *R. emiliae*, ▲ Specimens from north Goiás, west Tocantins, southern Piauí, western portion of Bahia and northern region of Minas Gerais.

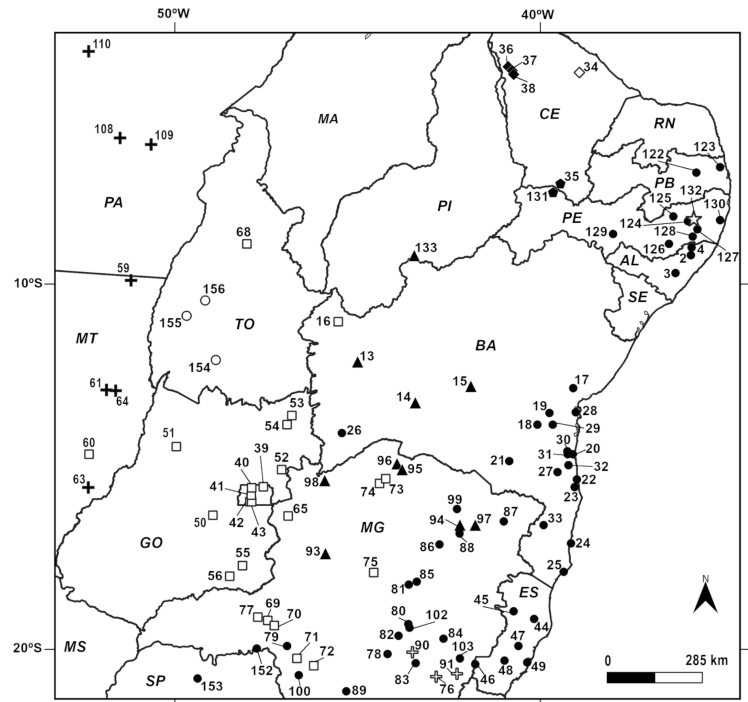


Figure 2 – Enlarged area delimited by a square in Fig. 1. Brazilian states acronyms are: AL=Alagoas, BA=Bahia, CE=Ceará, ES=Espirito Santo, GO=Goiás, MA=Maranhão, MG=Minas Gerais, PB=Paraíba, PE=Pernambuco, PI=Piauí, RN=Rio Grande do Norte, SE=Sergipe, TO=Tocantins. Numbers and species symbols as explained in Fig. 1.

Rhipidomys and discuss the phylogenetic relationships and taxonomic issues of the lowland forms of the “leucodactylus” section of the genus.

Materials and methods

Morphological analyses

We examined a total of 358 specimens, mainly skins and skulls, from 137 localities and deposited at the mammal collections of the following institutions: Museu de Zoologia da Universidade de São Paulo (MZUSP); Museu Nacional da Universidade Federal do Rio de Janeiro (MN); Universidade Federal do Espírito Santo (UFES); Universidade Federal de Minas Gerais (UFMG); Pontifícia Universidade Católica de Minas Gerais (PUC-MG); Universidade Federal de Pernambuco (UFPE); Universidade Federal da Paraíba (UFPB); The Natural History Museum, London (BMNH).

We studied specimens of all species of the Brazilian lowland “leucodactylus” section of *Rhipidomys* (Tribe, 2015), except *R. ipukensis* whose characters and measurements were retrieved from the original description (Rocha et al., 2011). For a more comprehensive comparison we also used information from the literature, mainly from contributions made by Tribe (2015); Costa et al. (2011); Rocha et al. (2011); Tribe (2005) and Allen (1916).

A list of the specimens examined is provided in Appendix B. A gazetteer including the Brazilian collecting localities of specimens of the “leucodactylus” section mentioned in this paper and on the revised literature is in Appendix C (see also Fig. 1 and 2). This study is in conformity to the ASM guidelines for the use of wild mammals in research and education (Sikes, 2016).

Qualitative analyses

To identify the different species, we employed morphologic characters currently being employed on the definition of species on Sigmodontinae (traits summarized in Tab. 2). We used the terminology of anatomical characters proposed by Steppan (1995); Voss (1993); Voss and Carleton (1993); Carleton and Musser (1989); Voss (1988); Reig (1977); Hershkovitz (1962) and Thomas (1910). These characters were used to recognize groups of specimens, based on their sharing of certain morphological patterns. Collecting localities of these groups of

specimens were plotted in maps together with localities mentioned in the literature (Fig. 1 and 2; Appendix C). This information was used for the recognition of geographic discontinuities and for discovering relations of sympatry or parapatry (as preconized by Vanzolini, 1993; Musser, 1968).

Quantitative analyses

The external measurements were obtained from the original labels of collectors. They are: total length (TL), tail length (T), hind foot length (HF); ear length (E), weight (W) (Tab. 1). Twenty-nine cranial and dental measurements were taken, under stereomicroscope when necessary, using a digital caliper, with 0.1 mm of resolution. They are taken as follows: Alveolar Upper Molar Row (AUMR), from the anterior-most point of the alveolus of M^1 to the posterior-most point of the alveolus of M^3 ; Braincase Breadth (BCB), taken at the joint of the temporo-parietal suture and the lambdoidal ridge; Bullar Length (BL), maximum length of the bulla, excluding the tube; Bullar Width (BW), maximum width of the bulla, between the middle of the medial side at the petrosal-basioccipital suture and the dorsal process of the ectotympanic; Breadth of Zygomatic Plate (BZP), breadth of zygomatic plate at mid-height; Condylar-Incisor Length (CIL); Crown Length of upper Molar Row (CUMR), from the most posterior point of the occipital condyles to the anterior border of the incisive alveolus; Diastema Length (DL), between the most posterior point of the border of the incisive alveolus and the most anterior point of the crown of M^1 ; Depth of Ramus (DR), least distance between the most upper point of the condylar process and the lowest point of the angular process; greatest length of skull (GL), the greatest length of the skull measured from the back of supraoccipital to the tips of the nasals; Greatest Length of Mandible (GLM), from the rearest point of the condylar process to the most anterior point of the incisive alveolus; Incisive Foramen Breadth (IFB), maximum breadth between external borders of both incisive foramina; Incisive Foramen Length (IFL), maximum internal length of the incisive foramen; Interorbital Breadth (IOB), least breadth across the frontal bones; Longitudinal Diameter of upper Incisor (LDI), antero-posterior diameter of upper incisor at the posterior border of alveolus; Length of lower Molar Row (LMR), from the front face of the crown of M^1 to the rear face of the crown of M^3 ;

Table 1 – Descriptive statistics of external, skull and mandible measurements (mm) and weight (g) of 13 Brazilian species of lowland *Rhipidomys* of the “leucodactylus” section. Mean±standard deviation, (minimum–maximum) and sample size for each variable. TL, total length; T, tail length; HF, hind foot length; E, ear length; W, weight; BCB, Braincase; BL, Bullar Length; BW, Bullar Width; BZP, Breadth of Zygomatic Plate; CIL, Condylo-Incise Length; DL, Diastema; DR, Depth of Ramus; GL, greatest length of skull; GLM, Greatest Length of Mandible; IFB, Incisive Foramen Breadth; IFL, Incisive Foramen Length; IOB, Interorbital Breadth; LDI, Longitudinal Diameter of upper Incisor; LMR, Length of lower Molar Row; MIB, M¹ Breadth; MFB, Mesopterygoid Fossa Breadth; NL, Nasal Length; PBI, Palatal Breadth at M; PB3, Palatal Breadth at M; PBL, Palatal Bridge Length; PL, Palatal Length; PPL, Post-Palatal Length; RB, Rostral Breadth; RL, Rostral Length; TDI, Transversal Diameter of upper Incisor; TFL, Temporal Fossa Length; AUMR, Alveolar Upper Molar Row; CUMR, Crown Length of upper Molar Row; ZB, Zygomatic Breadth.

	Samples from North GO, West TO, South PI, West BA and North MG		<i>R. mastacalis</i>	<i>R. cearanus</i>	<i>R. cariri</i>	<i>R. baturiteensis</i>	<i>R. macrurus</i>	<i>R. tribei</i>
	Samples from Bezerros							
HB	120±3.6 (117–124) 3	134±13.7 (103–148) 10	133.6±27.3 (97–300) 118	125.5±1.0 (94–185) 48	140.80±19.9 (110–190) 15	136.2±12.2 (110–154) 17	124.7±7.9 (113–130) 4	118±13.2 (96–130) 6
TL	275.6±9.2 (117–124) 3	302.5±30 (271–364) 10	290.8±33.4 (201–455) 118	286.3±29.7 (217–359) 48	309.8±34.3 (268–390) 15	306.1±36 (241–381) 17	281.2±19.2 (259–303) 4	261.5±18.5 (239–280) 6
T	155.6±6.8 (148–161) 3	168.5±22.9 (142–216) 10	158.6 ± 14.7 (124–200) 118	160.7±16.1 (120–210) 48	169±16.4 (140–200) 15	169.8±31.5 (120–254) 17	156.5±13.0 (146–173) 4	143.5±7.4 (134–150) 6
HF	30.3±0.5 (30–31) 3	26.6±2.1 (22–29) 10	27.0 ± 3.0 (17–42) 118	24.9±1.5 (22–30) 48	27.2±5.2 (20–37) 15	27.8±3.9 (20–38) 17	27.5±3.1 (23–30) 4	27.6±1.3 (25–29) 6
E	19.6±0.5 (19–20) 3	21.9±2.3 (19–27) 10	19.7±4.6 (12–62) 118	19.0±1.6 (13–21) 48	20.2±0.9 (19–23) 15	19.5±1.58 (17–22) 17	21.5±1.7 (20–24) 4	19.1±1.3 (18–21) 6
W	48±3 (45–51) 3	75.1±15.6 (53–105) 10	65.0±18.0 (20–115) 110	61.8±16.1 (27–92) 33	79.4±19.7 (38–120) 15	70.5±33.8 (35–180) 15	65.5±4.7 (61–72) 4	50.0±11.4 (36–67.5) 6
GL	31.7±0.6 (31.2–32.5) 3	33.6±1.7 (29.2–33.6) 20	33.2±1.5 (29–36.33) 123	32.8±1.8 (29.48–36.6) 46	34.5±1.4 (31.8–36.4) 12	34.2±1.7 (29.6–36.6) 16	33.6±1.8 (31.8–38.3) 10	31.4±1.7 (29.4–33.5) 5
CIL	28.4±0.8 (27.6–29.3) 3	30.6±1.9 (25.6–33.9) 21	30.0±1.4 (25.6–32.9) 125	29.9±1.85 (26.1–34.0) 47	31.7±1.6 (28.6–34.4) 12	31.2±1.5 (26.9–33.6) 16	30.6±1.6 (29.2–35.2) 11	28.2±1.4 (26.5–30.5) 6
PL	14.6±0.1 (14.4–14.8) 3	15.3±0.8 (13.2–16.7) 22	15.4±0.74 (13.2–16.9) 131	15.0±1.8 (13.3–17.1) 50	14.6±0.8 (13.8–17.1) 17	15.8±0.79 (13.9–16.9) 17	15.40±1 (14.1–17.9) 15	14.6±0.6 (13.8–15.6) 7
PPL	11.6±0.5 (11.0–12.1) 3	13.0±1.1 (10.1–13.0) 21	12.6±0.9 (9.8–14.7) 124	12.8±1 (10.6–15.0) 47	13.7±0.9 (12.1–15.2) 13	13.2±0.8 (11.3–14.5) 17	13.1±0.8 (12.2–15.6) 11	11.7±0.7 (10.6–12.5) 6
UMRC	5.5±0.0 (5.5–5.6) 3	5.0±0.1 (4.5–5.2) 22	5±0.1 (4.5–5.4) 119	4.9±0.1 (4.7–4.9) 50	5.1±0.1 (4.75–5.4) 17	5.4±0.1 (5.2–5.6) 18	5.1±0.1 (4.9–5.4) 14	4.8±0.1 (4.6–5.1) 7
UMRA	5.6±0.0 (5.6–5.7) 3	5.1±0.1 (4.7–5.6) 22	5.2±0.2 (4.7–6.4) 129	5.1±0.1 (4.7–5.8) 50	5.3±0.2 (4.8–5.8) 17	5.6±0.1 (5.3–5.8) 18	5.5±0.6 (5.0–7.7) 15	5.0±0.0 (4.9–5.2) 7
MIB	1.4±0.01 (1.4–1.4) 3	1.3±0.0 (1.2–1.4) 22	1.3±0.05 (1.2–1.5) 128	1.3±0.06 (1.2–1.5) 50	1.4±0.04 (1.3–1.5) 17	1.4±0.05 (1.4–1.6) 18	1.4±0.05 (1.2–1.5) 15	1.3±0.03 (1.3–1.4) 7
PBL	4.7±0.03 (4.7–4.8) 3	5.0±0.3 (4.5–5.7) 21	5.2±0.2 (4.6–6.5) 129	4.8±0.2 (4.3–5.4) 50	4.9±0. (4.4–5.5) 17	4.8±0.7 (2.1–5.6) 18	5.0±0.4 (4.5–6.0) 15	5.1±0.1 (4.8–5.4) 7
TFL	11.1±0.0 (11.0–11.2) 3	11.5±0.6 (9.7–12.6) 22	11.2±0.4 (9.8–12.6) 130	11.0±0.5 (9.7–12.3) 49	11.6±0.5 (10.5–12.6) 17	11.3±0.7 (9.6–12.1) 17	11.6±0.5 (11.0–12.8) 14	11.1±0.5 (10.3–11.7) 7
DL	7.8±0.1 (7.7–7.9) 3	8.4±0.6 (6.8–9.6) 22	8.5±0.5 (6.6–9.5) 127	8.3±0.6 (6.9–9.4) 50	8.6±0.6 (7.5–9.6) 17	8.7±0.6 (7.3–9.9) 17	8.4±0.6 (7.4–10.1) 15	7.9±0.5 (7.4–8.8) 7
IFL	6.8±0.04 (6.7–6.8) 3	6.7±0.5 (5.5–8.0) 22	6.4±0.4 (5.2–7.8) 129	6.6±0.4 (5.8–7.5) 50	7±0.4 (6.2–7.7) 17	7.3±0.5 (6.6–8.2) 17	6.7±0.4 (6–7.6) 15	6.1±0.3 (5.6–6.7) 7
IFB	2.6±0.0 (2.5–2.7) 3	2.5±0.2 (2.2–3.2) 22	2.5±0.2 (1.7–3.2) 128	2.6±0.2 (1.9–3.1) 50	2.6±0.1 (2.3–2.9) 17	2.6±0.1 (2.1–2.8) 17	2.8±0.1 (2.5–3.0) 15	2.6±0.1 (2.3–2.8) 7
PB1	3.1±0.1 (2.9–3.2) 3	3.3±0.2 (3.0–3.8) 22	3.4±0.2 (2.9–4.0) 116	3.3±0.1 (2.9–3.7) 50	3.6±0.2 (3.1–4.0) 17	3.4±0.2 (2.8–3.8) 18	3.4±0.2 (3.1–3.8) 15	3.3±0.1 (3.0–3.6) 7
PB3	3.3±0.16 (3.1–3.4) 3	3.7±0.3 (3.1–4.4) 22	3.7±0.2 (3.09–4.3) 113	3.5±0.2 (3.2–4.0) 50	3.9±0.2 (3.3–4.3) 17	3.8±0.1 (3.3–4.1) 18	3.7±0.2 (3.3–4.1) 12	3.6±0.1 (3.4–3.9) 7
MFB	1.9±0.1 (1.7–2.0) 3	2.0±0.2 (1.7–2.5) 22	2.0±0.1 (1.4–2.61) 129	1.9±0.1 (1.4–2.5) 50	2.2±0.2 (1.7–2.6) 16	2±0.2 (1.5–2.3) 18	2.1±0.2 (1.7–2.5) 15	2.0±0.06 (1.9–2.1) 7
TDI	1.7±0.0 (1.6–1.8) 3	1.9±0.1 (1.5–2.3) 22	2.0±0.1 (1.5–2.4) 127	2.0±0.2 (1.6–2.5) 49	2.0±0.1 (1.7–2.3) 17	2.1±0.1 (1.8–2.3) 16	2.1±0.2 (1.7–2.6) 15	1.9±0.1 (1.7–2.1) 7
LDI	1.7±0.02 (1.7–1.8) 3	1.8±0.1 (1.4–2.1) 22	1.8±0.1 (1.3–2.3) 126	1.8±0.1 (1.3–2.1) 48	1.9±0.1 (1.6–2.3) 17	1.8±0.1 (1.4–2.0) 17	1.8±0.2 (1.5–2.2) 14	1.7±0.1 (1.4–1.8) 7
BW	4.6±0.07 (4.5–4.7) 3	4.4±0.14 (4.1–4.7) 22	4.1±0.2 (3.7–5.2) 123	4.2±0.1 (3.9–4.5) 46	4.5±0.2 (4.1–5) 12	4.4±0.1 (4.1–4.8) 16	4.3±0.1 (4.2–4.5) 11	4.2±0.2 (4.0–4.6) 5
BL	4.6±0.06 (4.5–4.6) 3	4.4±0.1 (4.1–4.7) 22	4.0±0.2 (3.4–4.6) 124	4.0±0.2 (3.1–4.7) 46	4.3±0.3 (3.5–4.7) 12	4.3±0.1 (4.1–4.6) 14	4.1±0.1 (3.9–4.4) 11	4.2±0.2 (3.8–4.5) 5
BCB	11.2±0.3 (10.9–11.5) 3	11.3±0.5 (10.4–12.3) 22	11.7±0.4 (10.6–12.7) 124	11.3±0.4 (10.3–12.3) 46	11.4±0.4 (10.7–12.5) 14	11.4±0.3 (10.6–12.0) 16	11.5±0.4 (10.8–12.0) 12	12.0±0.2 (11.7–12.4) 6
RB	4.0±0.1 (3.8–4.0) 3	4.3±0.2 (3.8–5.0) 22	4.2±0.2 (3.6–5.0) 129	4.0±0.2 (3.5–4.8) 50	4.2±0.2 (3.6–4.7) 17	4.4±0.2 (3.9–4.8) 17	4.3±0.2 (4.0–4.9) 15	4.3±0.2 (3.9–4.7) 7
RL	10.7±0.5 (10.2–11.2) 3	11.7±0.8 (9.5–13.5) 21	11.2±0.7 (9.3–12.7) 125	11.0±0.8 (9.2–12.7) 48	12.1±0.8 (10.6–13.6) 16	11.7±0.8 (9.9–12.8) 17	11.6±0.9 (10.1–13.7) 12	10.4±0.7 (9.4–11.6) 6
NL	10.5±0.3 (10.1–10.8) 3	11.2±0.9 (9.1–12.6) 21	11.1±0.7 (9.2–12.6) 125	11.0±0.8 (9.0–13.3) 48	11.4±0.7 (9.7–12.8) 16	11.5±0.8 (9.6–13.0) 17	11.0±0.9 (9.5–12.7) 13	10.1±0.7 (9.3–11.3) 6
BZP	3.2±0.3 (2.9–3.6) 3	2.9±0.2 (2.0–3.3) 22	2.9±0.7 (2.2–11.1) 129	2.8±0.3 (2.2–3.5) 50	3.0±0.2 (2.7–3.6) 17	3.1±0.2 (2.6–3.6) 18	3.4±2.2 (2.4–11.3) 14	2.6±0.2 (2.4–3.0) 7
IOB	5.2±0.1 (5.0–5.3) 3	5.1±0.2 (4.7–5.7) 22	5.3±0.2 (4.6–6.1) 130	5.1±0.2 (4.5–8.9) 50	5.4±0.2 (4.4–5.8) 17	5.2±0.2 (4.6–5.7) 18	5.3±0.3 (4.6–6.0) 15	5.2±0.1 (5.0–5.4) 7
ZB	13.3±2.1 (10.9–14.8) 3	14.7±0.5 (13.7–15.5) 21	14.8±0.6 (12.9–16.1) 129	14.7±0.6 (13.8–16.8) 48	15.5±0.9 (14.0–17.2) 15	15.5±0.7 (13.4–16.6) 16	14.9±0.5 (14.5–15.9) 12	14.7±0.5 (13.8–15.4) 7
GLM	16.8±0.3 (16.4–17.2) 3	18.1±0.9 (16.1–19.8) 22	18.0±0.7 (15.8–19.7) 129	17.6±0.8 (15.8–19.8) 50	18.3±0.9 (16.3–19.8) 17	18.1±0.8 (16.5–19.2) 16	18.3±0.9 (17.1–20.7) 14	17.3±0.6 (16.5–18.2) 7
LMR	5.8±0.09 (5.8–5.9) 3	5.2±0.1 (4.8–5.6) 22	5.2±0.1 (4.8–5.7) 120	5.2±0.1 (4.9–5.6) 50	5.3±0.2 (4.6–5.7) 17	5.7±0.1 (5.4–6.0) 17	5.4±0.1 (5.1–5.7) 15	5.2±0.1 (5.0–5.5) 7
DR	5.3±0.1 (5.1–5.4) 3	5.9±0.4 (4.9–6.7) 22	5.8±0.3 (4.9–6.6) 128	5.8±0.3 (4.9–5.6) 50	6.1±0.4 (5.5–6.8) 17	5.8±0.3 (5.2–6.5) 17	5.9±0.3 (5.3–6.5) 13	5.5±0.3 (5.2–6.0) 7

M¹ Breadth (**MIB**), maximum breadth of the crown across the middle of M¹; Mesopterygoid Fossa Breadth (**MFB**), maximum breadth of the mesopterygoid fossa; Nasal Length (**NL**), greatest length of the nasal; Palatal Breadth at M¹ (**PB1**), measured across the hard palate on the lingual surface of the M¹ crowns; Palatal Breadth at M³ (**PB3**), measured across the hard palate on the lingual surface of the M³ crowns; Palatal Bridge Length (**PBL**), from the posterior end of the incisive foramen to the posterior edge of the bony palate excluding any medial postpalatal process; Palatal Length (**PL**), from the anterior-most point of the incisive alveolus to the posterior edge of the bony palate excluding any medial postpalatal process; Post-Palatal Length (**PPL**), from the posterior edge of the bony palate excluding any medial postpalatal process to the ventral margin of the foramen magnum; Rostral Breadth (**RB**), breadth of rostrum above the infraorbital foramen; Rostral Length (**RL**), length of rostrum between the posterior border of the maxillary root of the zygomatic arch and the tip of the nasal; Transversal Diameter of upper Incisor (**TDI**), transversal diameter of upper incisor taken just above the wear surface; Temporal Fossa Length (**TFL**), maximum length of the orbito-temporal fossa, taken in dorsal view, between the posterior border of the maxillary root and the anterior border of the squamosal root of the zygomatic arch; greatest length of upper molar row measured on the crowns of M¹ and M³; Zygomatic Breadth (**ZB**), greatest breadth of the zygomatic arches at the squamosal root.

Age and sex variation

To compare the morphologic and morphometric variation of the specimens examined (semaphoronts), we classified the available skulls into age classes based on the eruption and differential wear of molars (Fig. S6): Age Class A is composed of young specimens, whose third upper molar (M3) is not completely erupted; Age Class B composed of young adults and adults, with dentine exposed at occlusal surface, but main enamel features of the molar crown (anteromedian flexus, anteroloph, mesoloph, and posteroloph) still distinguishable; and Age Class C composed of older individuals, with molars greatly worn, with major exposition of dentine, and most features of crowns no longer distinguishable (Percequillo, 1998; Brandt and Pessoa, 1994; Oliveira, 1992; Voss, 1991). For all morphometric and morphological analysis, we employed only individuals of the Age Class B. We tested sexual dimorphism with adult specimens of this class, through a two-sample t-test using the cranial measurements listed in Tab. 1.

Molecular analyses

We employed cytochrome b (Cytb) sequence of 70 specimens of 14 species of the genus *Rhipidomys* available in NCBI database (Genbank), plus 11 new sequences from specimens hypothesized to represent the new species herein (Appendix A); these represent the “leucodatyus”, “macconnelli” and “fulviverter” sections of the genus. The species *Reithrodon auritus* (Genbank: EU579474), *Rhagomys rufescens* (Genbank: AY206770), and *Thomasomys aureus* (Genbank: U03540) were used as outgroups.

The mtDNA of the new sequences was extracted from tissues samples of liver or muscle preserved in 96% ethanol. We utilized the Kit Wizard Genomic DNA Purification (Promega) according to the manufacturer’s instructions. The DNA extracted was amplified in Biocycler-Bioystems thermal cycler with MVZ 05 (light-strand – CGAAGCTTGATATGAAAAACCATCGTTG) and MVZ 16 (heavy-strand – AAATAGGAARTATCAYTCTGGTTTRAT) primers as suggested by (Smith and Patton, 1993). Amplification was made with denaturation at 93 °C for 2 min, annealing at 45 °C for 1.5 min, and extension at 72 °C for 2 min, with 32 cycles for double-stranded and 35 cycles for single-stranded amplification (Smith and Patton, 1993). The PCR products were purified with exonuclease I and shrimp alkaline phosphatase (American Biosciences) and direct sequenced with the ABI Prism Big Dye Terminator Cycle Sequencing Ready Reaction Kit (Perkin Elmer Applied Biosystems) according to the manufacturer’s instructions. The sequences were obtained using an ABI3500 automatic DNA sequencer. The final product of sequencing consisted of 500-801 base-pair sequences of Cytb.

The sequences were checked and aligned with Bioedit 7.0.8.0 (Hall, 1999), and the DNASP 5.10.01 (Librado and Rozas, 2009) was used to generate the haplotype database. The evolutionary model was checked in ModelGenerator v.0.85 (Keane et al., 2006). We employed two optimality criteria to evaluate the phylogenetic relationships for species of genus, Maximum Likelihood (ML) and Bayesian Inference (BI) methods. The ML topology was reconstructed with the Nearest Neighbor Interchange and Subtree Pruning and Regrafting algorithm with five BioNJ initial random trees (Guindon et al., 2010; Guindon and Gascuel, 2003). The supports were obtained with the approximate likelihood test Shimodaira-Hasegawa-like interpretation (SH-aLRT), considered conservative and requiring less time than bootstrap (Anisimova et al., 2011; Guindon et al., 2010). The BI was conducted in Mr.Bayes on the CIPRES portal (Miller et al., 2010) with 10000000 generations registered every 100 and the first 10% discarded as burn-in. The convergence was checked through the Tracer 1.5 program (Rambaut et al., 2014). Both trees were edited in FigTree 1.4.3 (Rambaut, 2016) and GIMP (The GIMP Development Team, 2019).

Molecular species delimitation analysis

We estimated species limits within *Rhipidomys* employing the Poisson Tree Process model (bPTP) (Zhang et al., 2013). This model is mainly intended to single-locus molecular phylogenies by evaluating the number of substitutions between and within species (Zhang et al., 2013). We used as input the tree from the ML analysis with *Thomasomys aureus* as outgroup. The bPTP analysis was performed on the web server (<https://species.h-its.org/ptp/>) with 500000 Monte Carlo Markov-Chain (MCMC) generations and the remaining parameters set by default. The convergence is checked in Tracer 1.5 program (Rambaut et al., 2014); we employed both the ML solution and the highest Bayesian supported solution.

Statistical analysis and species limits

The groups recognized by molecular data, morphological character analysis and by geographic distribution were assigned to different “species”, including the new species here hypothesized. To test the hypothesis of this arrangement, at first, we checked data normality by multivariate analyses of Mardia and Kurtosis in PAST program (Hammer et al., 2001) for the proper choice of a parametric or nonparametric analysis. Since the data exhibit normal distribution, we performed a Canonical Discriminant Analysis (CDA) (Hair et al., 2007). We included samples of groups from the Brazilian northeastern region, geographically close to the distribution of the new species. The CDA methods maximize differences between groups and minimize the differences within groups (Hair et al., 2007; Reis, 1988), an approach adequate for our purposes, as we are using qualitative and molecular data to define the groups to be tested.

Specimens of the species of genus *Rhipidomys* from Northeastern Brazil are rare in collections and hard to be obtained in the field, with few specimens available. To evaluate if the small samples from some localities could be biasing the results of the CDA, we performed one additional Principal Component Analysis (PCA). This exploratory technique considers the variables without any prediction of dependent variables, with no *a priori* restriction (Hair et al., 2009). Further, a non-parametric multivariate analysis of variance with permutation (perMANOVA) was performed in PAST (Hammer et al., 2001). This method was applied to test if the species recognized by us was correctly classified. We used as metric the distance of Mahalanobis and a pairwise post-hoc test was performed with *p*-values with uncorrected significance.

The results of molecular, morphological qualitative and quantitative approaches were integrated (Dayrat, 2005) for the recognition of species limits, in an approach that attends the criteria of the phylogenetic species concept, with the identification of diagnosable monophyletic lineages Cracraft (1983).

Table 2 – Geographical distribution and skull characters of 13 Brazilian species of lowland *Rhipidomys* of the “leucodactylus” section.

Characters	Samples from						Range
	Samples from Bezerros	North GO, West TO, South PI, West BA and North MG	<i>R. mastacalis</i>	<i>R. cearanus</i>	<i>R. cariri</i>	<i>R. baturiteensis</i>	
1-Geographical distribution (Fig. 1, 2)	Type locality	North Goiás, west Tocantins, east Piauí, west Bahia and north Minas Gerais	East Brazil, from Paraíba to Rio de Janeiro	Serra de Ibiapaba, north CE	Chapada do Araripe	Baturité	Range northeast CE
2-Nasolacrimal capsule ^a (Fig.4, 6, S3)	Less inflated	Inflated	Inflated	Less inflated	Inflated	Less inflated	
3-Tip of nasals vs. tip of premaxilar ^b (Figs. 4, 6, 8, S3)	In front	In front	In front	At level	In front	At level	
4-Lateral border of nasals ^c (Figs. 4, 8, S3)	Slightly flared ventrally	Strongly flared ventrally	Slightly flared ventrally	Slightly flared ventrally	flared ventrally	Slightly flared ventrally	
5- Shape of the zygomatic notch ^d (Figs. 4, S3)	Shallow	Deeper	Deeper	Shallow	Deeper	Deeper	
6- Interorbital breath ^e (Figs. 4, S3)	Larger	Smaller	Larger	Larger	Smaller	Smaller	
7-Angle of frontal ridges ^f (Figs. 4, S3)	More convergent	Less convergent	More convergent	More convergent	Less convergent	Less convergent	
8- Shape of the incisive foramina ^g (Figs. 4, 7, S3)	Bullet	Bullet	Ellipse	Ellipse	Bullet	Bullet	
9- Shape of the borders of mesopterygoid fossa ^h (Figs. 4, 7, S3)	“M” or “U”	“3”	“M”	“M” or “U”	Horseshoe	“U”	
10- Position of the posterior border of the palatal bridge ⁱ (Figs. 4, 7, S3)	Shorter-M ³ mesoloph	Shorter- M ³ posterior border	Shorter-M ³ mesoloph	Shorter-M ³ mesoloph	Shorter-M ³ mesoloph	Shorter- M ³ posterior border	
11- Position of the posterior end of the incisive foramina in relation to first molar ^j (Figs. 4, 7, S3)	Longer	Shorter	Shorter	Longer	Longer	Longer	
12- Position of the bulla in lateral view related to the level of the upper molar series ^m (Figs. 4, 8)	More inflated and bulky	Small bulla	Small bulla	Small bulla	Small bulla	Small bulla	
13- Form of the dorsal profile of the skull ⁿ (Figs. 4, 8)	Rounded	Straight	Rounded	Rounded	Straight	Straight	
14- Parapterygoid fossa Depth ^o (Figs. 4, S3)	Shallow	Excavated	Shallow	Shallow	Excavated	Shallow	

^a The nasolacrimal capsule may be inflated widening the rostrum at this place or less inflated. The nasolacrimal foramen may be corresponding larger or smaller.

^b The tip of the nasals at the level of the anterior process of the premaxilar or further in front the premaxillary.

^c Outer border of the distal third of the nasal bones strongly flared ventrally or less flared ventrally.

^d Zygomatic notch in dorsal view shallow or slightly deeper.

^e Interorbital breath larger or smaller.

^f Frontal ridges more convergent or less convergent.

^g Outer borders of the incisive foramina is evenly concave (ellipse) or parallel posteriorly and convergent in anteriorly (teardrop shaped or bullet shaped).

^h Mesopterygoid fossa widened anteriorly with the palatine and the postpalatal process forming a “3” shaped aspect; moderate widened anterior with less convergent posteriorly, with the palatine and the postpalatal process forming a “M” shaped aspect; moderate widened anterior with less convergent posteriorly and parallel sided, “U” Shaped, the postpalatal process when present is very inconspicuous; Mesopterygoid fossa widened anteriorly and convergent posteriorly with a horseshoe shape.

ⁱ Palate shorter, not reaching the posterior border of M3 alveolus; reaching half of M3 (mesoloph); or longer reaching the posterior border of the alveolus.

^j Incisive foramina longer reaching or slightly trespassing the anterior border of M1 alveolus; or shorter not reaching the alveolus.

^m Bulla inflated and bulky, trespassing the molar series in lateral view; or small bulla slightly trespassing the molar series in lateral view.

ⁿ Dorsal profile of skull in lateral view straight in the anterior 2/3 and sloping down in the posterior 1/3; or the whole dorsal profile evenly rounded.

^o Deep excavated or shallow excavated dorsally in ventral view.

Results

Morphological analyses

Sorting specimens according to the characters (Tab. 2) revealed the existence of 13 morphological groups (Fig. 4–8, S3). Comparing the diagnostic features of these groups with: i) nominal taxa original descriptions, ii) with characters attributed to species in the literature (Tribe, 2015; Costa et al., 2011; Rocha et al., 2011; Tribe, 2005; Allen, 1916), and iii) with the geographic distribution of the type localities and of the current known species, we attributed to each of these groups a valid species name. Some samples from Brazil are distinct qualitatively from other congeneric forms of the lowland “leucodactylus” section, and we

believe that there are no available names for them: one sample from Bezerros, in Pernambuco, and several samples from Goiás, Tocantins, Piauí, Bahia and Minas Gerais (see Tab. 2 and Fig. 4–8, S3).

Multivariate comparisons

We did not find sexual dimorphism within species (results not shown); therefore both sexes were pooled in samples. For the statistical multivariate comparative analyses, we employed samples of other species of *Rhipidomys* from Northeastern Brazil, distributed near the presumed range of the two new species, namely *R. cariri*, *R. baturiteensis*, *R. mastacalis* and *R. cearanus*. The canonical discriminant analyses show

Table 2 – Geographical distribution and skull characters of 13 Brazilian species of lowland *Rhipidomys* of the “leucodactylus” section (continued).

Characters	<i>R. “macrurus”</i>	<i>R. ipukensis</i>	<i>R. tribei</i>	<i>R. itoan</i>	<i>R. leucodactylus</i>	<i>R. nitela</i>	<i>R. emiliae</i>
1-Geographical distribution (Fig. 1, 2)	Minas Gerais, Goiás, Distrito Federal, Mato Grosso do Sul and Paraguai	C Tocantins	MG SE	E SP and RJ	Peru, Equador, Colombia, Venezuela and Brazilian Amazon	Guiana and adjacent land	High- and low- Amazonia Basin
2-Nasolacrimal capsule ^a (Fig. 4, 6, S3)	Less inflated	Less inflated	Less inflated	Inflated	Inflated	Inflated	Less inflated
3-tip of nasals vs tip of premaxilar ^b (Figs. S3)	At level	In front	In front	In front	At level	At level	In front
4-Lateral border of nasals ^c (Figs. 4, 8, S3)	Slightly flared ventrally	Strongly flared ventrally	Slightly flared ventrally	Slightly flared ventrally	Slightly flared ventrally	Slightly flared ventrally	Slightly flared ventrally
5- Shape of the zygomatic notch ^d (Figs. 4, S3)	Shallow	Deeper	Shallow	Shallow	Shallow	Shallow	Shallow
6- Interorbital breath ^e (Figs. 4, S3)	Smaller	Larger	Larger	Larger	Smaller	Smaller	Larger
7-Angle of frontal ridges ^f (Figs. 4, S3)	More convergent	More convergent	More convergent	More convergent	Less convergent	Less convergent	More convergent
8- Shape of the incisive foramina ^g (Figs. 4, 7, S3)	Bullet	Ellipse	Bullet	Tear-drop	Bullet	Bullet	Bullet
9- shape of the borders of mesopterygoid fossa ^h (Figs. 4, 7, S3)	“M”	“M”	“U”	“U”	“U”	“U”	“M”
10- position of the posterior border of the palatal bridge ⁱ (Figs. 4, 7, S3)	Shorter-M ³ mesoloph	Short - M ³ border	Long	Long	Long	Long	Shorter – M3 posterior border
11- position of the posterior end of the incisive foramina in relation to first molar ^j (Figs. 4, 7, S3)	Shorter	Shorter	Longer	Longer	Shorter	Longer	Shorter
12- Position of the bulla in lateral view related to the level of the upper molar series ^m (Figs. 4, 8)	Small bulla	Small bulla	Small bulla	Small bulla	Small bulla	Small bulla	Small bulla
13- Form of the dorsal profile of the skull ⁿ (Figs. 4, 8)	Straight	Straight	Straight	Straight	Straight	Straight	Straight
14-Parapterygoid fossa Depth ^o (Figs. 4, S3)	Excavated	Shallow	Shallow	Shallow	Shallow	Shallow	Excavated

^a The nasolacrimal capsule may be inflated widening the rostrum at this place or less inflated. The nasolacrimal foramen may be corresponding larger or smaller;

^b The tip of the nasals at the level of the anterior process of the premaxilar or further in front the premaxillary;

^c Outer border of the distal third of the nasal bones strongly flared ventrally or less flared ventrally;

^d Zygomatic notch in dorsal view shallow or slightly deeper;

^e Interorbital breath larger or smaller;

^f Frontal ridges more convergent or less convergent;

^g Outer borders of the incisive foramina is evenly concave (ellipse) or parallel posteriorly and convergent in anteriorly (teardrop shaped or bullet shaped);

^h Mesopterygoid fossa widened anteriorly with the palatine and the postpalatal process forming a “3” shaped aspect; moderate widened anterior with less convergent posteriorly, with the palatine and the postpalatal process forming a “M” shaped aspect; moderate widened anterior with less convergent posteriorly and parallel sided, “U” Shaped, the postpalatal process when present is very inconspicuous; Mesopterygoid fossa widened anteriorly and convergent posteriorly with a horseshoe shape;

ⁱ Palate shorter, not reaching the posterior border of M3 alveolus; reaching half of M3 (mesoloph); or longer reaching the posterior border of the alveolus;

^j Incisive foramina longer reaching or slightly trespassing the anterior border of M1 alveolus; or shorter not reaching the alveolus;

^m Bulla inflated and bulky, trespassing the molar series in lateral view; or small bulla slightly trespassing the molar series in lateral view;

ⁿ Dorsal profile of skull in lateral view straight in the anterior 2/3th and sloping down in the posterior 1/3th; or the whole dorsal profile evenly rounded;

^o Deep excavated or shallow excavated dorsally in ventral view.

small overlaps on the multivariate space of selected species (Fig. 9), and the highest discriminant values were obtained between the first and second canonical variates (Tab. S5). These results suggest that the qualitative traits used above were useful for the delimitation of diagnosable groups, as the most discriminatory variables in the first canonical root were CIL, IFL, NL and RL, related to the overall skull length and rostrum length, as well as the mandibular length. The variables that resume most of the variation on the second canonical root were DR, PPL, DL, LMR, that are also associated to skull length and mandibular size (Tab. S5). These variables reflect the skull size and more specifically the morphological variation found in rostrum, including the incisive foramina, of the examined specimens. Samples from Bezerros appears isolated from the other species, both on the first and second function, as well as *Rhipidomys baturiteensis*. Samples from Piauí, Bahia and Minas Gerais also appear as a distinct cluster of individuals, separated

from all other known species, and slightly overlapping to specimens of *R. cariri* and *R. cearanus*.

The PCA showed that samples of Bezerros (n=3) do not overlap with other samples in the multivariate space, and even the ellipse with the confidence interval appears distant from the clouds of specimens of other species studied. Most of the remaining samples overlap along the PC1, but across the PC2 it is possible to see the tendency of separation between the clouds of specimens of geographic samples (Fig. S7). The first two components accounted for about 55% of the total variation, and the variables that contributed most were Breadth of Zygomatic Plate (BZP), Diameter of Incisor (DI), Post Palatal Length (PPL) and Rostral Length on PC1; and Bullar Length (BL), Bullar Width (BW), Incisive Foramina Length (IFL) and Breadth of Zygomatic Plate (BZP) on PC2. The perMANOVA results showed that all species recognized in morphological analysis were significantly different of each other, ex-

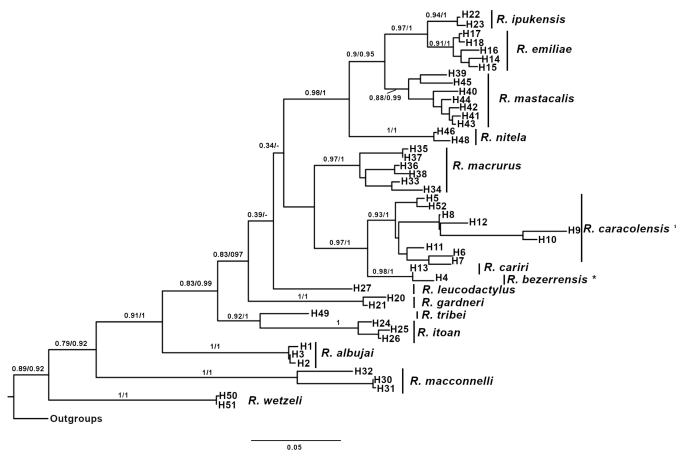


Figure 3 – Phylogenetic position of the *Rhipidomys* samples from Bezerros and the samples from north Goiás, west Tocantins, Piauí, West Bahia and North Minas Gerais based on cytochrome b sequences. The topology corresponds to MV method. The branch labels shows the SH-aLRT and Posterior Probability (PP) respectively. The branches with a dash indicates the polytomy of IB topology (Supplementary Data SD1 and SD2).

cept *R. baturiteensis* and samples from Southern Piauí, Western Bahia and Northern Minas Gerais (Tab. S8).

Molecular analyses and species delimitation

The best estimated model for base pairs substitutions was HKY+G. The topologies of both approaches, ML and BI, are similar and recovered a strong monophyletic group of *Rhipidomys* (0.86/0.92) that includes 15 clades (composed by the available species sequences in the Genbank plus the samples from Bezerros and the samples from Northern Goiás, Western Tocantins, Southern Piauí, West Bahia and North Minas Gerais (Fig. 3). The two phylogenies differ only regarding the position of *R. leucodactylus* (Fig. 3, S1 and S2). This species appears as sister of a clade formed by *R. ipukensis*, *R. emiliae*, *R. mastacalis*, *R. nitela*, *R. macrurus*, the samples from Southern Piauí, Western Bahia and Northern Minas Gerais, *R. cariri* and the specimens of Pernambuco (with low support) in the ML analysis or as a polytomy with all these species in the BI approach. The samples from Pernambuco correspond to a unique haplotype (Appendix A), sister group to *R. cariri*. These two taxa are grouped together with the Northern Goiás, Western Tocantins, Southern Piauí, Western Bahia and Northern Minas Gerais specimens.

The bPTP analysis recovered 14 species for the ML tree for both methods (ML solution and Highest Bayesian supported solution), similarly to the 15 clades obtained in ML and BI approaches: the samples from Northern Goiás, Western Tocantins, Southern Piauí, Western of Bahia, and Northern Minas Gerais are estimated as a unique valid species; on the other hand, the samples from Bezerros grouped together with *R. cariri* as one species; moreover, the valid species *R. ipukensis* and *R. emiliae* were also considered as a single species; *R. macconnelli* was split as two different species (Fig. S4), and the remaining 9 clades were recovered as species, as currently established in the literature (Brito et al., 2017; Tribe, 2015), namely *R. leucodactylus*, *R. gardneri*, *R. wetzeli*, *R. albujai*, *R. nitela*, *R. tribei*, *R. itoan*, *R. macrurus* and *R. mastacalis*.

The combination of shape and size variation, along with the phylogenetic relationships employing cyt b, suggest that the samples from Bezerros, in Pernambuco and the samples from Goiás, Piauí, Minas Gerais and Bahia represent distinct new species of the genus. We present extensive descriptions and detailed comparisons, coupled to comparisons with information available on the literature for this group, aiming to emphasize these differences and the uniqueness of these taxa.

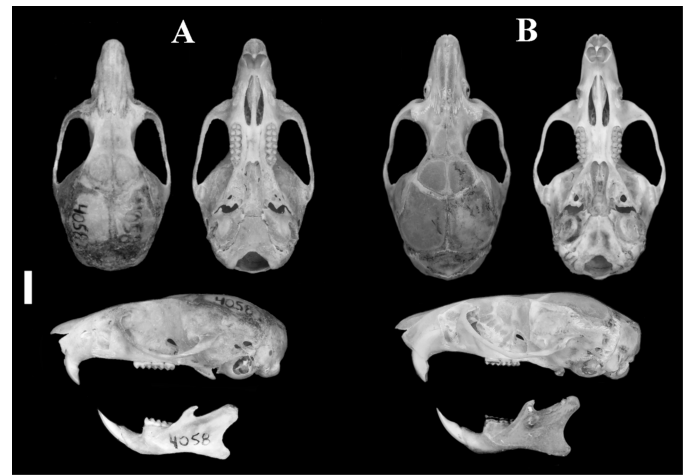


Figure 4 – Dorsal, ventral and lateral views of the skull and mandible of the holotypes of (A) *R. bezzerensis* sp. nov. (UFPB 4058) and (B) *R. caracolensis* (MZUSP 35687). Scale bar: 5 mm.

Systematic account

Rhipidomys bezzerensis sp. nov. Campos, B.A.T.P.; Percequillo, A.R.; Langguth A.

Bezerros Climbing tree rat
(Tab. 1 and 2; Fig. 4–8; S3)

Holotype: UFPB 4058 (Fig. 5 and 6); the holotype consists of an undamaged skin and skull of an adult female, collected by Francisco Oliveira Filho, original number FO 15, on April 18, 2002. The external measurements (in mm) are: HB=119, T=161, HF=32, E=20, W=45 g. See skull measurements in Tab. 1.

Type Locality: Vertentes, Municipality of Bezerros, Pernambuco state, Brazil (8°11'35" S, 35°47'31" W; altitude 770 m) (Fig. 2).

Paratypes: We assign as paratypes the follow specimens, all from type locality: Female: UFPB 4057, UFPB 4060, UFPB 6563; Males: UFPB 4059, UFPB 4061 (see Material Examined, Appendix B).

Distribution: *Rhipidomys bezzerensis* is known only from the type locality (Fig. 2). Bezerros is located at the Serra da Borborema, a highland oriented north-south, about 100 km parallel to the Brazilian coast. In this area, moisture carried by trade winds is retained orographically allowing the presence of wet forests enclaves, known locally as “Brejos de Altitude” (see Andrade-Lima, 1982); these are considered priority areas of conservation by the Ministério do Meio Ambiente (Brasil,

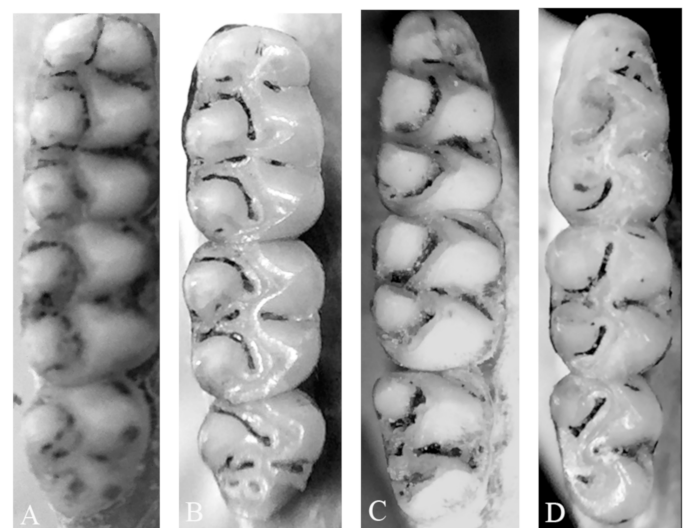


Figure 5 – Upper and lower molar rows of *R. bezzerensis* UFPB 4058 (A, B) and *R. caracolensis* MZUSP 35687 (C, D).

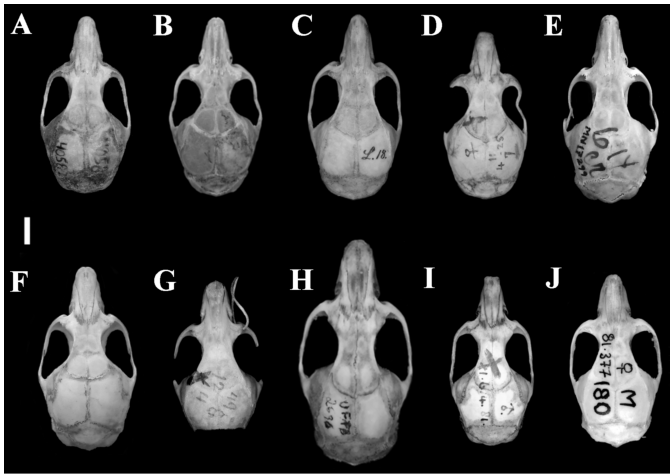


Figure 6 – Dorsal view of skulls of ten species of *Rhipidomys*. A: *R. bezerrensis* (holotype UFPB 4058), B: *R. caracolensis* (holotype MzUSP 35687), C: *R. mastacalis* (holotype ZMUC.L. 16), D: *R. cearanus* (holotype BMNH 11.4.25.7), E: *R. cariri* (MN 17299), F: *R. baturiteensis* (MRT 78), G: *R. macrurus* (cotype BMNH 491284), H: *R. leucodactylus* (UFPB 2696), I: *R. nitela* (holotype BMNH 1. 6.4.81), J: *R. emiliae* (BMNH 81.377). Scale bar: 5 mm.

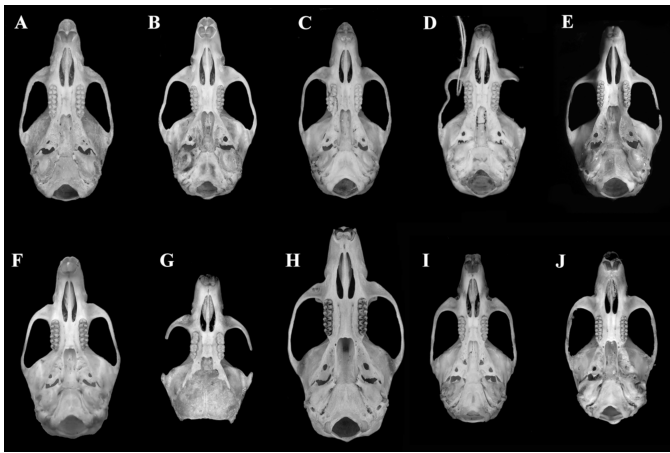


Figure 7 – Ventral view of skulls of ten species of *Rhipidomys*. Letters identify species as in Fig. 6. Scale bar: 5 mm.

2018) due high human impact on these areas. Bezerros are geographically near other “Brejos” of the state of Pernambuco (n=6), localities where, so far, *R. mastacalis* was the only species of the genus ever recorded (Fig. 2: points 127–130), as Parque Estadual Vasconcelos Sobrinho (40 km apart) and Brejo da Madre de Deus (distant nearly 70 km), based the series of specimens of genus *Rhipidomys* housed at the UFPB collection (see Specimens Examined, Appendix A).

Etymology: The name *bezerrensis* refers to the type locality, in the municipality of Bezerros, Pernambuco state.

Diagnosis: *Rhipidomys bezerrensis* is characterized by the following unique combination of morphological traits: nasal bone long and narrow, with the distal third less flared ventrally; dorsal surface of nasal bone flat, not accompanying the premaxillary curvature; premaxillary inflated and robust with, a narrow nasolacrimal canal opening; supraorbital margins longer extending farther cranially; dorsal profile of braincase rounded; large, inflated and bulky auditory bulla, more ventrally positioned than the occipital bones.

Description: Small sized species of genus *Rhipidomys*, with adult head-and-body length ranging from 114 to 124 mm; tail length ranging from 148 to 161 mm; pes length ranging from 30 to 31 mm; ears length from 19 to 20 mm; weight ranging from 45 to 51 g. Dorsal pelage moderately long, soft; pelage brownish-greyish, with a grizzled overall appearance; base of dorsal hairs dark gray, with the pheomelanin portion of the aristiforms restricted to the top (final quarter) in dark brown, long (range: 12–14 mm) and thin; setiforms (range: 8–9 mm) and viliforms

hairs (range: 5–6 mm) shorter and thin and with apical third with dark yellow color. Ventral coloration white to cream, with variably present pectoral spots of self-colored hairs; ventral hairs self-colored or dark gray color at the base. Mystacial vibrissae thick, dense and long, reaching 40 mm at maximum; vibrissae dark brown. Tail longer than head and body (126% to 135% of head and body length), with a short pencil (8 mm); tail scales, squared and imbricated in an annular arranged series; scales with three short and thick hairs, not reaching the next adjacent row of scales; scales and hairs brown, dorsally and ventrally. Pinnae short and rounded, frequently with long brown hairs in the inner distal surface. Pes long (range: 30 to 31 mm), broad, with very conspicuous dark patch on the dorsal surface of the metatarsal region, reaching the digits; patch pelage with very few golden hairs; long digits with white unguet tuft barely reaching the distal portion of the claws.

Skull of moderate size (Fig. 4–6; Tab. 1). Rostrum long and robust; nasal bones with lateral margins less flared ventrally, and projecting well beyond premaxillaries. Zygomatic notch very shallow and narrow, with nasolacrimal projection positioned outside the notch and not expanded. Lacrimal small and rounded, in contact with the frontal. Zygomatic arches slightly divergent posteriorly; moderately robust. Interorbital region with supraorbital margins strongly divergent posteriorly; margins sharp and acute, not forming a ridge. Braincase elongated, with well-marked squared dorsolateral margins, configuring a moderately rounded profile; lambdoidal and occipital crest very weak, configuring a more rounded occipital region. Gnathic process present, not well projected beyond incisors. Nasolacrimal capsule moderately inflated, with a narrow lacrimal foramen. Zygomatic plate narrow, with free dorsal margins slightly projected anteriorly, and anterior margin straight; maxillary root of zygomatic arch broad. Zygomatic arch moderately thin. Alisphenoid strut robust, configuring separate openings for the oval foramen and the masticatory-buccinator foramen. Carotid circulatory pattern III (Voss, 1988). Hamular process of squamosal robust, dividing a small postglenoid foramen and a larger subsquamosal fenestra. Auditory bullae well inflated, with large external auditory meatus; tegmen tympani developed, overlapped to the suspensory process of squamosal; mastoid rounded, with large fenestra. Dorsal profile of skull evenly rounded in lateral view. Incisive foramina long and

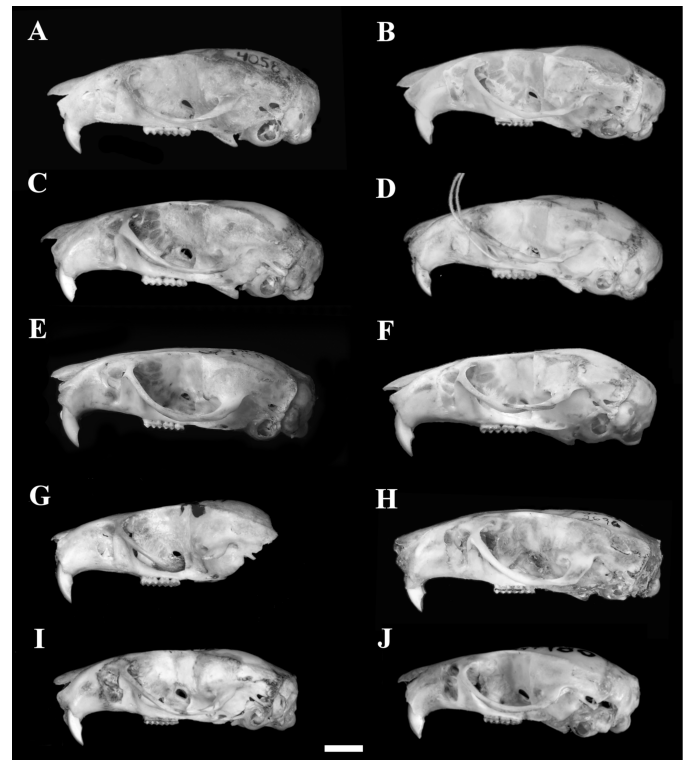


Figure 8 – Lateral view of skulls of ten species of *Rhipidomys*. Letters identify species as in Fig. 6. Scale bar: 5 mm.

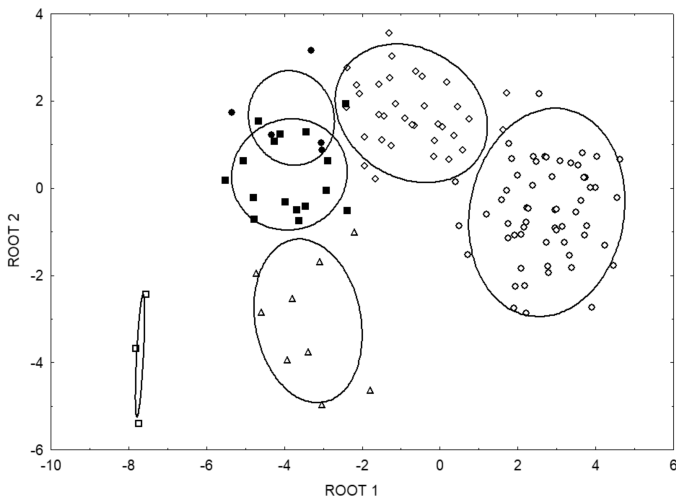


Figure 9 – Canonical Discriminant Analyses for species of *Rhipidomys* from Brazilian Northeast. Ellipses indicate 95% confidence intervals. Species symbols are: \diamond *R. cearanus*, \square Specimens from Bezerros, \triangle *R. baturiteensis*, \bullet *R. cariri*, \blacksquare Specimens from southern Piauí, western portion of Bahia and northern region of Minas Gerais, \circ *R. mastacalis*.

wide; posterior margin reach the alveolus of M^1 ; lateral margins wider posteromedially, configuring a very long “bullet shaped” foramina. Palate wide and short; anterior margin of mesopterygoid fossa penetrates between molar series, reaching the hypoflexus of M^3 ; fossa moderate with lateral margins wide anteriorly, less convergent posteriorly and parallel sided, “U” or “M” shaped; a small postpalatal process may be present. Roof of fossa completely ossified; palate with small and simple posterolateral palatal pits. Parapterygoid plates wide, with the same width that mesopterygoid fossa; posterior opening of alisphenoid canal small; medium lacerate foramen large. Auditory bullae very rounded, bulked and inflated; bony eustachian tube wide and short; bullae projected more ventrally than the molar series; periotic capsule of mastoid very inflated.

Mandible with coronoid process large and falciform, nearly equal in height to condyloid process, angular process short, not surpassing the condyloid process posteriorly; the capsular process of the lower incisor is prominent and lies just below the coronoid process or the anterior part of the sigmoid notch.

Upper incisors ophistodont; incisors with anterior enamel band orange. Upper molar series with long and robust molars; molar crowns low brachyodont; main cusps arranged in predominantly opposite pairs, although lingual cusps are slightly anterior to the labial ones; labial and lingual flexi not very deep, bending posteriorly, penetrating only slightly at molar midplane. First upper molar with procingulum slightly narrower than paracone-protocone pair; anteromedian flexus present and deep, dividing the antercone in two equal-sized conules in some individuals; the caudal end of the flexus is oriented labially; anteroloph present, posterior to anterolabial conule, parallel to it and separated from it by shallow anteroflexus; anteroloph connected to anterior mure; paracone connected posteromedially to protocone, and both connected to the median mure by a small lophule; paracone separated from the protocone by a deep paraflexus; paracone with a distinct anterolabial style, almost forming a lophule (as there are two parallel anterolophes); protocone connected anteriorly to anterior mure and separated from anterolingual conule through a deep and wide protoflexus; mesoloph long and narrow, connected with mesostyle labially, and to the median mure medially; paracone with or without a small and oblique paralophule, connected at the middle portion of the mesoloph, defining a small and medial mesofossette; mesoloph separated from metacone by a deep metaflexus; metacone linked posteromedially to hypocone; hypocone connected to median mure anteriorly and separated from protocone by a deep and very wide hypoflexus; posteroloph developed, reaching lingual margin; small posterofossette present (in young specimens; quickly eroded in subadult and adult specimens). Second upper molar with anterior mure present; anteroloph present, connected to the

anterior mure; anterolingual cingulum absent; paracone connected to the median mure posteromedially, configuring a long labial paraflexus; paracone connected labially to mesoloph through a paralophule, forming a labial mesofossette; an additional oblique paralophule may be present on the medial portion of mesoflexus (or mesofossette), forming a medial and small mesofossette; two small mesofossettes could be present on upper second molar; mesoloph well developed, originating from the median mure and fused to mesostyle; hypoflexus wide and deep, without lingual style; metacone connected to the labial portion of posteroloph, not connected to the hypocone; posteroloph long, reaching the labialmost portion of molar; hypocone well developed. Third upper molar reduced; anteroloph visible, linked anteromedially to anterior mure; anterolingual cingulum absent; paracone connected posteromedially to median mure; mesoloph well developed, reaching the labial rim; paracone fused labially to the mesoloph; metacone reduced, fused to the mesoloph anterolabially, to the posteroloph posterolabially, and to the median mure anteromedially; hypocone small, connected to the posteroloph; hypoflexus deep and wide, oriented anteriorly, deeply separating the protocone and hypocone.

Lower incisors long and narrow, with enamel band yellow-orange; molar series with cusps in opposite pairs. First lower molars with procingulum narrower than metaconid-protoconid pair; anteromedian flexid absent; internal fossetid defines two conulids, equal in size; anterolophid small; anterolingual cingulid fused to anteroloph and to the labial margin of the metaconid; anterolabial cingulid well developed, connected to procingulum, separated from the protoconid by a deep and wide protoflexid; metaconid and protoconid joined anteromedially to the anterior murid; metaconid connected to the anterolophid by a small medial metalophulid, defining a separation of the metaconid from the anterolophid by two anterofossetids; protoconid connected medially to the median murid; protoconid separated to the metaconid by a deep and wide mesoflexid; mesolophid long and narrow, connected to the mesostylid, distinct; mesolophid separated of the entoconid by a narrow entoflexid; entoconid connected medially to the hypoconid, and also to the mesolophid by two entolophulids, forming two small entofossetids; posterolophid originating at posterior end of hypoconid and extending almost to lingual side of the molar; short and wide posteroflexid. Second lower molar similar to first lower molar; anteroconid absent; anterolabial cingulid present; metaconid and protoconid anteromedially united by anterior murid; protoconid separated from anterolabial cingulum by protoflexid and hypoconid by hypoflexid; mesolophid long, fused or not to protoconid (mesolophid absent on 22% of specimens); entoconid and hypoconid connect to the median murid anteromedially; entoconid fused to the mesolophid by a entolophulid, forming an oblique entofossetid. Lower third molar smaller than third upper molar; anterolabial cingulid present; metaconid and protoconid developed, separated by mesofossetteid; hypoconid separated from protoconid by hypoflexid; entoconid reduced, indistinguishable from the mesolophid and posterolophid.

Natural History: *Rhipidomys bezerrensis* apparently is endemic to the Brejos de Altitude of Bezerros, Pernambuco. The forests of the municipality are currently reduced and very anthropized. The specimens were sampled during the Projeto de Conservação e Utilização Sustentável da Diversidade Biológica Brasileira — PROBIO project that aimed to study the “Brejos de Altitude” from Pernambuco and Paraíba states at the end of the 1990’s (de Sousa et al., 2004).

Remarks: Tribe (2015, 2005, 1996) did not examine these specimens from Bezerros, but Costa et al. (2011) and Costa (2007) examined and identified them as *R. mastacalis*. The few specimens from Bezerros were probably overlooked and misidentified as *R. mastacalis*, as this is the most common species of *Rhipidomys* from Paraíba and Pernambuco “Brejos de Altitude” available in UFPB (Appendix B). It is interesting to point that the type locality of *R. bezerrensis* is about 40 km from Caruaru, where only *R. mastacalis* was collected (Fig. 2) in an intensive sampling effort. In the Comparisons section below, we present data to support the discrimination between those two species, despite their close geographic proximity. Specimens of *R. bezerrensis* were retrieved as the sister species of *R. cariri* (Fig. 3 and Appendix A) in a

separate lineage of specimens of other Paraíba and Pernambuco “brejos” that were assigned as *R. mastacalis* (Fig. 4; Appendix C). Considering the endemism, few specimens collected and anthropogenic pressure in the Brejos de Altitude this species is probably in risk of extinction (see below).

***Rhipidomys caracolensis* sp. nov.** Campos, B.A.T.P.; Percequillo, A.R.; Languth, A.

Caracol Climbing tree rat
(Tab. 1 and 2; Fig. 4–8, S3)

Rhipidomys sp.: Costa et al. (2011, 958)

Rhipidomys macrurus (sensu Tribe, 1996): Tribe (2015, 606)

Rhipidomys sp. 1: Rocha et al. (2011, 23, Fig. 13)

Rhipidomys mastacalis cytotype 1: Andrades-Miranda et al. (2002) and Paixão et al. (2021, 4, Tab. 1)

Rhipidomys mastacalis cytotype 2: Andrades-Miranda et al. (2002) and Paixão et al. (2021, 4, Tab. 1)

Holotype: MZUSP 35687; the holotype is an adult female collected by Alexandre Reis Percequillo (original field number ARP 152), January 22, 2002. The holotype consists of an undamaged skin, skull and partial skeleton (Fig. 4); tissue preserved in ethanol 90%. The external measurements (in mm) are: HB=139, T=198, HF=30, E=26, W=70 g.

Paratypes: We assign as paratypes the following specimens, all from the type locality: Females: MZUSP 35683, MZUSP 35685, MZUSP 35688, MZUSP 35689, MZUSP 35690, MZUSP 35691, MZUSP 35692; Males: MZUSP 35682, MZUSP 35684, MZUSP 35686 (see Material Examined, Appendix A).

Distribution: *Rhipidomys caracolensis* is known from six localities in southern Piauí, western portion of Bahia and northern Minas Gerais, in Brazil (Fig. 1 and 2; Appendix B, Appendix C for more information).

Etymology: The name *caracolensis* refers to the Municipality of Caracol, in the Piauí state.

Diagnosis: *Rhipidomys caracolensis* is characterized by a unique combination of morphological traits: nasal bones longer and narrower than in other *Rhipidomys* with a narrow and rounded tip, with lateral projection at the distal third strongly flared ventrally; premaxillary bone is inflated and robust with a moderate nasolacrimal foramina breath; the interorbital region has a sharp convergence in medial portion, with slightly posterior divergence and weak supraorbital ridge. The dorsal profile of the skull is straight in the anterior 2/3 and sloping down in the posterior third (convex). Incisive foramina are bullet-shaped, short, not reaching M^1 root. Mesopterygoid fossa is broad in anterior portion, and reach M^3 root; the outline is like a number three (3) with the open part facing down.

Description: Medium sized species of the genus *Rhipidomys* with adult head-and-body length ranging from 103–148 mm and tail length ranging 142 to 216 mm. Dorsal pelage brownish-yellowish, with an agouti overall appearance. Aristiforms hairs thin, light brown (range: 12–15 mm), setiforms (range: 6–10 mm) and viliforms hairs (length 5–8 mm) with 4th basal portion light gray, tips ochre. Ventral coloration varies from white to cream, with variably present pectoral spots; ventral hairs self-colored or dark gray color at the base. Mystacial vibrissae thin, long and in low density, reaching 52mm in maximum length. Tail longer than head and body (103% to 145% of head and body length), with a short length pencil (maximum length 4 mm); tail scales, squared and imbricated in an annular arranged series; scales with three short and thick hairs, not reaching the next subjacent row of scales; scales and hairs brown, dorsally and ventrally. Pinnae short and rounded, frequently with long brown hairs in the inner distal surface. Ears large, with few and short light brown hair in the internal surface. Hind foot small (range: 22 to 29 mm), broad with the dark metatarsal patch well defined; patch pelage are streaky by several golden hairs; digits short with unguet tufts white and not too dense.

Skull of moderate size; rostrum of medium length (Fig. 4, 6–8, S3; Tab. 1); nasal bone with expanded sides, far surpassing the premaxillary bone; outer border of distal third of the nasal bones strongly flared

ventrally. Zygomatic notch in dorsal view slightly deeper with nasolacrimal projection positioned outside the notch and not expanded; lacrimal bone small and rounded in contact with frontal bone; zygomatic arches slightly divergent posteriorly, robust. Interorbital region with a more anterior convergence and slightly posterior divergence, with a smooth frontal bone crest in the distal portion. Braincase elongated, with rectangular dorsolateral margins; lambdoidal crest pronounced configuring a longer occipital region. Gnathic process present, not well projected beyond incisors. Nasolacrimal capsule inflated with the lacrimal foramen narrow. Zygomatic plate extended slightly anterior and do not reach the nasolacrimal capsules, zygomatic root large and in angle to the skull. Alisphenoid strut robust, configuring separate openings for the oval foramen and the masticatory-buccinator foramen. Carotid circulatory pattern III (Voss, 1988). Hamular process of squamosal thin, dividing a very small postglenoid foramen almost occluded by the process and a larger subsquamosal fenestra; dorsal profile of skull is straight in the anterior 2/3 and sloping down in the posterior 1/3 in lateral view. Incisive foramina shorter and wide posterior, not reaching the alveolus of M^1 ; lateral margins wider posteromedially and parallel, configuring bullet-shaped foramina. Palate shorter and wide anteriorly; anterior margin of mesopterygoid fossa just reaches the posterior border of M^1 alveolus; fossa widened anteriorly and very convergent posteriorly, “3” shaped; a small postpalatal process may be present. Roof of fossa completely ossified; palate with no posterolateral palatal pits; parapterygoid plates wider than the width of mesopterygoid fossa; posterior opening of alisphenoid canal large; medium lacerate foramen large. Auditory bullae small and not inflated; bony eustachian tube is thin and delicate in lateral view.

Mandible with coronoid process large and falciform, nearly equal in height to condyloid process, angular process short, not surpassing the condyloid process posteriorly; the capsular process of the lower incisor is prominent and lies just below the coronoid process or the anterior part of the sigmoid notch. Upper incisors opistodont, with anterior enamel band orange. Upper molar series with long and robust molars; molar crowns low brachyodont; main cusps arranged in predominantly opposite pairs, although lingual cusps are slightly anterior to the labial ones; labial and lingual flexi deep, obliquely oriented, moderately penetrating at molar midplane. First upper molar with procingulum slightly narrower than paracone-protocone pair; anteromedian flexus present and deep, dividing the anterocone in two equal-sized conules in some individuals; the caudal end of the flexus is oriented labially; anteroloph present, posterior to anterolabial conule, parallel to it and separated from it by shallow anteroflexus; anteroloph connected to anterior mure; paracone connected posteromedially to protocone, and both connected to the median mure by a small lophule; paracone separated from the protocone by a deep paraflexus; paracone with a distinct anterolabial style, almost forming a lophule (as if there are two parallel anterolophes); protocone connected anteriorly to anterior mure and separated from anterolingual conule through a deep and wide protoflexus; mesoloph long and narrow, connected with mesostyle labially, and to the median mure medially; paracone with or without a small and oblique paralophule, connected at the middle portion of the mesoloph, defining a small and medial mesofossette; mesoloph separated from metacone by a deep metaflexus; metacone linked posteromedially to hypocone; hypocone connected to median mure anteriorly and separated from protocone by a deep and very wide hypoflexus; posteroloph developed, reaching lingual margin; small posterofossette present (in young specimens; quickly eroded in subadult and adult specimens). Second upper molar with anterior mure present; anteroloph present, connected to the anterior mure; anterolingual cingulum absent; paracone connected to the median mure posteromedially, configuring a long labial paraflexus; paracone connected labially to mesoloph through a paralophule, forming a labial mesofossette; an additional oblique paralophule may be present on the medial portion of mesoflexus (or mesofossette), forming a medial and small mesofossette; two small mesofossettes could be present on upper second molar; mesoloph well developed, originating from the median mure and fused to mesostyle; hypoflexus wide and deep, without lingual style; metacone connected to the labial por-

tion of posteroloph, not connected to the hypocone; posteroloph long, reaching the labialmost portion of molar; hypocone well developed. Third upper molar reduced; anteroloph visible, linked anteromedially to anterior mure; anterolingual cingulum absent; paracone connected posteromedially to median mure; mesoloph well developed, reaching the labial margin; paracone fused labially to the mesoloph; metacone reduced, fused to the mesoloph anterolabially, to the posteroloph posterolabially, and to the median mure anteromedially; hypocone small, connected to the posteroloph; hypoflexus deep and wide, oriented anteriorly, deeply separating the protocone and hypocone.

Lower incisors long and narrow, with enamel band yellow-orange; molar series with cusps in opposite pairs. First lower molars with procingulum narrower than metaconid-protoconid pair; anteromedian flexid absent; internal fossetid defines two conulids, equal in size; anterolophid small; anterolingual cingulid fused to anteroloph and to the labial margin of the metaconid; anterolabial cingulid well developed, connected to procingulum, separated from the protoconid by a deep and wide protoflexid; metaconid and protoconid joined anteromedially to the anterior murid; metaconid connected to the anterolophid by a small medial metalophulid, defining a separation of the metaconid from the anterolophid by two anterofossetids; protoconid connected medially to the median murid; protoconid separated to the metaconid by a deep and wide mesoflexid; mesolophid long and narrow, connected to the mesostylid, distinct; mesolophid separated of the entoconid by a narrow entoflexid; entoconid connected medially to the hypoconid, and also to the mesolophid by two entolophulids, forming two small entofossetids; posterolophid originating at posterior end of hypoconid and extending almost to lingual side of the molar; short and wide posteroflexid. Second lower molar similar to first lower molar; anteroconid absent; anterolabial cingulid present; metaconid and protoconid anteromedially united by anterior murid; protoconid separated from anterolabial cingulum by protoflexid and hypoconid by hypoflexid; mesolophid long, fused or not to protoconid (mesolophid absent on 22% of specimens); entoconid and hypoconid connect to the median murid anteromedially; entoconid fused to the mesolophid by a entolophulid, forming an oblique entofossetid. Lower third molar smaller than third upper molar; anterolabial cingulid present; metaconid and protoconid developed, separated by mesofosseteid; hypoconid separated from protoconid by hypoflexid; entoconid reduced, indistinguishable from the mesolophid and posterolophid.

Natural History: Parque Nacional da Serra das Confusões is one of the best-preserved conservation units of the Caatinga Biome (Gregorin et al., 2008). Specimens were sampled in two occasions, on September/October 2000 and on January 2002. The inventory sampled all habitats present on the Park (Gregorin et al., 2008), but specimens were trapped only in the moist forest remnants, which are located on narrow and deep valleys, associated to sandy rocky formations (see also Dal Vechio et al., 2016 for information for the habitats). Although some trees were deciduous, this forest remains green throughout the year, even on the dry season, when all species of the surrounding Caatinga are leafless (Gregorin et al., 2008). One individual was obtained from the stomach contents of a colubrid snake (*Drymarchon corais*), captured at the transition between the forest and an old abandoned orchard with fruit trees.

Remarks: Costa et al. (2011) and Costa (2007) identified some specimens from Bahia, Goiás, Minas Gerais and Tocantins as *Rhipidomys* sp. 3 and *Rhipidomys* sp., respectively, and noticed that they may represent an unnamed species. We examined some of those specimens and identified them as *Rhipidomys caracolensis*. The specimens not examined by us may also belong to the new species since they group together in Costa et al. (2011) and Costa (2007) phylogenies. Besides that, the sequences of these specimens grouped together within type series material of *R. caracolensis* (PNSC) in our phylogeny (Fig. 3). Thomazini (2013) stated that specimens from Coronel Murta and Formoso (Minas Gerais) and Andaraí (Bahia), exhibited the karyotype $2n=44/FN=50$ and pointed out that de Sousa (2005) obtained the same karyotype for specimens from PNSC, the type locality of *R. caracolensis* (specimens examined in this study). Paixão et al. (2021) ana-

lysed karyotypes from Andrades-Miranda et al. (2002) from Colinas do Sul, Minaçu, Uruaçu and Niquelândia. In both works are assigned as *R. mastacalis* with two cytotypes $2n=44/FN=76$ and $2n=44/FN=80$. Paixão et al. (2021) provisionally allocated these specimens as *R. mastacalis* by the high FN, but pointed that may correspond to *R. ipukensis*. The sequences of these specimens are used in our molecular analyses and grouped in the same clade with samples from northern Goiás, western Tocantins, South Piauí, West Bahia and North Minas Gerais, as well as a distinct species by bPTP analyses, and, thus, we considered these samples as *R. caracolensis*. Rocha et al. (2011) employed one of the specimens from Coronel Murta in their phylogenetic analysis of *Rhipidomys*, naming it as *Rhipidomys* sp. 1; we examined this specimen and we identified it as *R. caracolensis*. Tribe (2015) provisionally allocated specimens from phylogenetic works of Costa et al. (2011); Costa (2007) and Costa (2003) as *R. macrurus*. Here, we demonstrate that all these specimens represent a new species.

Based on these results, we hypothesize that *R. caracolensis* exhibit a wide distribution, not necessarily restricted to forest enclaves in Caatinga, such as Serra das Confusões, but possibly also occurring in gallery forests within the Cerrado domain, as indicated by samples from Coronel Murta.

Comparisons: We compared the specimens of *R. bezerrensis* from Pernambuco and *R. caracolensis* from Piauí, Bahia and Minas Gerais with specimens of the lowland section of the genus *Rhipidomys* (Tribe, 2015) (Tab. 1 and 2). Like most other Brazilian species of *Rhipidomys*, *R. bezerrensis* and *R. caracolensis* do not exhibit a single diagnostic autapomorphic character. Instead, they are diagnosed by unique combinations of character states that are operational and useful for species recognition (Tab. 2). In general, the most valuable character datasets to differentiate *Rhipidomys* species are in the skull, since external morphology is quite variable with overlapping sets of characters. The most diagnostic character to differentiate *R. bezerrensis* from the others congeneric Brazilian species is the inflated and voluminous auditory bulla, while the diagnostic character for *R. caracolensis* is the shape of mesopterygoid fossa (Tab. 2).

Samples of *R. bezerrensis* and *R. caracolensis* are smaller than *R. leucodactylus*, the largest species of the genus, whose head and body length often exceed 180mm and occipito-nasal length (ONL) usually greater than 40 mm (Tribe, 2015) (Fig. 6–8; Tab. 2). *Rhipidomys leucodactylus* also exhibits conspicuous and large aristiforms and the tail tuft is very dense and long (15 mm), in contrast with *R. bezerrensis* and *R. caracolensis*, which have shorter tufts (modal length: 8 and 4 mm, respectively). These few traits are sufficient to discriminate *R. leucodactylus* from other Brazilian species.

Regarding general size, specimens from Bezerros are smaller in head and body length (HB) than most species, being only larger than *R. tribei* (Tab. 1). On the other hand, specimens of *R. caracolensis* exhibit large head and body length, being smaller only than *R. cariri*, *R. itoan* and *R. baturiteensis*, besides *R. leucodactylus*. Specimens from Bezerros exhibit the largest hind foot, with longer digits (besides *R. leucodactylus*), while specimens of *R. caracolensis* present smaller feet, larger only than *R. ipukensis*, *R. cearanus* and *R. nitela*.

R. bezerrensis differ from *R. mastacalis* in dorsal pelage. The former is grayish-brown while the latter is orange-brown or reddish-brown. Additionally, *R. bezerrensis* possess a less inflated nasolacrimal capsule, while in *R. mastacalis* it is more inflated. The zygomatic notch of the sample from Bezerros is shallow in contrast to the deeper one in *R. mastacalis*. The incisive foramen exhibits a long bullet shape, with the posterior margin reaching M^1 , while in *R. mastacalis* the foramen is shorter not reaching M^1 , with an elliptical shape. Finally, the most diagnostic character of *R. bezerrensis* is the bulky and inflated bullae, which differentiate this species from *R. mastacalis* and all other.

The other species geographically close to the sample from Bezerros is *R. cariri*, from Crato (Ceará). The two species are quite distinct: *R. cariri* is much larger and exhibits brownish-yellowish coloration, when compared to the smaller grayish-brown individuals from Bezerros. Cranially, these species are also very distinct, with *R. bezerrensis* exhibiting a less inflated nasolacrimal capsule, a shallow zygomatic

notch, parapterygoid fossa shallow and the shape of the anterior border of mesopterygoid fossa “M” or “U” shaped. On the other side, *R. cariri* shows an inflated nasolacrimal capsule, deep zygomatic notch, anterior border of mesopterygoid fossa in “horseshoe” shape and an excavated parapterygoid fossa (see Tab. 2; Fig. 4–8, S3).

Specimens from Piauí, Bahia and Minas Gerais that represents *R. caracolensis* occur near the distribution of *R. ipukensis*, *R. “macrurus”* and *R. mastacalis*. *R. caracolensis* specimens are in average larger than these nearby distributed species (Tab. 1; see also Rocha et al., 2011: 25, Tab. 3). The best character to distinguish *R. caracolensis* specimens from the other Brazilian *Rhipidomys* is the shape of mesopterygoid fossa which is widened anteriorly with the palatine and the postapalatal process forming a “3” shaped profile. In contrast, all the other three nearby species possess an “M” shaped profile.

Specimens assigned to *R. caracolensis* differ from known individuals of *R. ipukensis* in several cranial characters. On the rostrum, the nasolacrimal capsules are less inflated, while specimens of *R. ipukensis* have a more inflated capsule; the interorbital breadth is narrow with less convergent ridges whilst *R. ipukensis* possess larger, more convergent interorbital ridges; the incisive foramina of *R. caracolensis* is bullet shaped contrasting with the ellipse-shape of *R. ipukensis*; the parapterygoid fossa is deep and excavated rather than shallow as in *R. ipukensis*.

Rhipidomys caracolensis differs from *R. mastacalis* by external and cranial characters. It has a yellowish-brown dorsal coloration that resembles *R. ipukensis* and *R. cariri*, but is quite different from the orange-reddish pelage exhibited by *R. mastacalis*. *R. mastacalis* and *R. ipukensis* possess similarities in the rostrum, interorbital region, shape of incisive foramina, mesopterygoid and parapterygoid fossae, that sets them apart from *R. caracolensis*. The first two, exhibit less inflated nasolacrimal capsules, large interorbital breath, with the angles of the frontal ridges more convergent, as well as a “M” shaped mesopterygoid fossa, while the specimens of *R. caracolensis* have inflated nasolacrimal capsules, smaller interorbital breath and a distinct mesopterygoid fossa “3” shaped. Specimens of *R. caracolensis* and *R. cariri* resembles each other in the fur color, but differs in the mesopterygoid fossa, the first species possess a “3” shape, while the last one has a horseshoe shape. Besides that, *R. cariri* is easily distinguished from the new species by its larger size, longer incisive foramina, nasals not projected downwards, and the nasolacrimal foramen very inflated and projected laterally.

The specimens assigned by Tribe (2015) as *R. “macrurus”* — in quotes because they exclude the ones we recognize as *R. caracolensis* sp. nov. — are quite different from those of *R. caracolensis*: the nasolacrimal capsule is less inflated; the tip of nasals bone is at the same level of the premaxillary, with lateral borders slightly flared ventrally setting a short, and wide rostrum aspect, while the new species has an inflated nasolacrimal capsule with the tips of the nasal bones ending in front of the premaxillary with a strongly flared ventrally projection configuring a more slender rostrum; the zygomatic notch of *R. “macrurus”* is shallow, contrasting with *R. caracolensis* that has a deeper aspect; the interorbital region is smaller and the angle of frontal ridges is more convergent while the new species has a narrow interorbital region but with less convergent ridges; the anterior margin of the mesopterygoid fossa reaches the M³ mesoloph while in *R. caracolensis* the anterior margin just reaches the M³ posteroloph.

The samples of *R. bezerrensis* resemble *R. baturiteensis* by the presence of a long incisive foramina, but in the latter species, these foramina are even longer, surpassing the anterocone of M¹. The two species also share the similar mesopterygoid fossa shapes. Besides that, the skull of Bezerros samples are very different, with a shallow zygomatic notch, larger interorbital breath and with the ridges of frontal more convergent, unlike *R. baturiteensis*, which exhibits a deeper zygomatic notch and a smaller interorbital breadth with less convergent angles of frontal ridges; this portion of frontals is evenly rounded in *R. baturiteensis*. The samples of *R. caracolensis* are easily distinguishable from *R. baturiteensis* by the horseshoe shape of the mesopterygoid fossa, and the flared ventrally distal portion of the nasal. *R. baturiteensis* on the con-

trary exhibits a “U” shaped mesopterygoid fossa and a nasal bone with little lateral downwards projection.

The specimens of Bezerros when compared with specimens of *R. cearanus* from Serra de Ibiapaba (Ceará) are smaller, with the nasal bones in front of the premaxillary, the incisive foramina are bullet shaped and the auditory bullae are inflated. The specimens of the second species possess the nasal bones at level of the premaxillary, with ellipse-shaped incisive foramina and small bullae (Tab. 2). Moreover, specimens of *R. caracolensis* have larger head-and-body size than specimens of *R. cearanus*.

Discussion

The diversity of genus *Rhipidomys*

The two new species described here, *Rhipidomys bezerrensis* sp. nov. and *R. caracolensis* sp. nov., increase the diversity of the “leucodactylus” section of the genus. These species were recognized based on molecular, morphologic and morphometric characteristics, that clearly distinguish them from other congeneric taxa. The present contribution assigns Linnean names to species provisionally identified (Tribe, 2015, 1996) under different informal names, as we mentioned in the remarks sections of the species accounts and discussed further below in this section.

The specimens from Bezerros, Pernambuco state, were only examined morphologically by Costa et al. (2011) and Costa (2007), and until now, no molecular data were available. Consequently, those specimens were misclassified as *R. mastacalis*. Here, we demonstrate based on several morphological traits that these specimens belong to another taxon, *R. bezerrensis*. Besides that, our phylogenetic analysis shows that *R. mastacalis* and *R. bezerrensis* belong to distant lineages. The first is related to species distributed in moister areas (Amazonia and Atlantic Forest) while the second is associated with the Open Dry Diagonal (Cerrado and Caatinga enclaves). Although the specimens that we recognize as *R. bezerrensis* and those of typical *R. cariri* (Crato specimens) were identified as a single species in bPTP analysis, the morphological and morphometric analysis clear shows sharp differences between specimens supporting our hypothesis. Both species are found only in Brejos, islands of moist forest surrounded by semiarid vegetation (Caatinga) (Andrade-Lima, 1966; Ab’Sáber, 2003; Tabarelli and Santos, 2004): as species of *Rhipidomys* are humid forest arboreal rats, we believe that these samples are definitely isolated geographically, reinforcing our hypothesis, since dispersal between such distant areas is unlike and the several nearby brejos of Bezerros harbor only *R. mastacalis* (Fig. 2). The Brejos of Pernambuco and Paraíba was extensively sampled (Pôrto et al., 2004) and yet, *R. bezerrensis* was just sampled in Bezerros, Pernambuco.

Other issue that deserves note is that bPTP analyses could be biased by the lack of a more comprehensive database of DNA sequences for the genus, including other species of “leucodactylus section” — *R. baturiteensis* and *R. cearanus* — as well as more sequences per species (Ahrens et al., 2016). It is important to highlight that Zhang et al. (2013) point that the species delimited by bPTP are putative only and additional data needs to be integrated to further validate the delimitation results, such as morphological characters. In this way, Vitecek et al. (2017) points that species delimitation are not sufficient yet to replace classical methods, as morphology. In this matter, we recognized *R. cariri* (specimens from Crato, Ceará) and *R. bezerrensis* as distinct species.

In the phylogenetic analysis recovered by Costa et al. (2011: 954, Fig. 8), specimens from Caratinga, Coronel Murta (Minas Gerais); Andaraí (Bahia); Paranã (Tocantins) and Serra da Mesa (Goiás) were assigned to *Rhipidomys* sp., a sister species to *R. cariri*, from Crato (Ceará). Later, Tribe (2015) allocated these specimens from drier areas referred as *Rhipidomys* sp. to *R. macrurus* and comment that these specimens likely represent an undescribed species. Here, we included samples from Serra das Confusões (Piauí) to the concept of this entity and formally described and named it as *R. caracolensis* sp. nov. This species was recognized in all analysis (morphological, morphometric and bPTP analysis).

Tribe (2005, 1996) recognized the specimens from Serra de Ibiapaba as *R. macrurus*, but later Tribe (2015) relocate these specimens as *R. mastacalis* (Lund, 1840) based on the sharing of fundamental number (FN=70) with specimens of *R. mastacalis* from Pernambuco and Bahia. However (see Tab. 1 and 2), we suggest that specimens from Ibiapaba are morphologically and morphometric different from *R. mastacalis*, and we suggest that the name to be employed to these specimens is *R. cearanus* Thomas 1910, a decision that we share with Paixão et al. (2021) and with Gurgel-Filho et al. (2015).

Tribe (2005) described two new subspecies under *Rhipidomys cariri*, *R. c. cariri* and *R. c. baturiteensis* from two isolated localities in the state of Ceará. Morphological and morphometrics differences between both populations are well documented in the original description and in this contribution (Tab. 2). We consider them different species, since no gradual geographic variation was reported by Tribe (2015) supporting gene flow between both ecologically isolated localities. Moreover, these taxa are clearly diagnosable, and the concept of subspecies would not be properly applied in this case (see Frost et al., 1992). Therefore, with the two new species described in this paper, along with the change on the status of *cariri* and *baturiteensis*, we raise the number of species of the “leucodatylos” section to 19 species, however, no molecular data is available for specimens from Baturité.

The *macrurus* issue

The identity of *R. macrurus* is uncertain and the new species described here and also other specimens of the genus, including a co-type of *macrurus* from the BMNH, offer new insights.

A brief history of the name is important to contextualize the changes throughout the history. Gervais (1855: 111) described *Mus (Hesperomys) macrurus* sp. nov., for a specimen from Crixás, Goiás collected by Castelnau and Deville. Later, Thomas (1886) stated that *macrurus* and *mastacalis* were true *Rhipidomys*, and later Thomas (1906), after discussing the characters of *Rhipidomys*, confirmed the inclusion of *H. macrurus* in this taxon. Later, Gyldenstolpe (1932: 46) considered *R. macrurus* a full species. Tate (1932: 19) included *macrurus* in the *Rhipidomys* group distributed over Brazilian Northeast and Mato Grosso. Cabrera (1961: 423) recognized all Brazilian *Rhipidomys* species under *R. mastacalis* with various subspecies, one of them *R. m. macrurus* but without information on its distribution. Musser and Carleton (1993: 745) followed Cabrera’s (1961) opinion, allocating most Brazilian species, including *R. macrurus*, under the synonymy of *R. mastacalis*; but it is important to notice that the synonyms of Musser and Carleton (2005, 1993) included not only taxa that are true junior synonyms but also subspecific names. Up to this date, taxonomic considerations regarding *R. macrurus* were not based on new material obtained in the field. Later, new specimens were collected and identified as “*macrurus*” but the name was not consistently applied by authors and may refer to different species.

Tribe (1996: 241), in an unpublished thesis, revised the genus and suggested for *R. macrurus* a distribution throughout the Brazilian Cerrado. He included in his concept of this species samples from Barreiras and Bom Jesus da Lapa, Bahia. Later, Costa (2007) and Costa et al. (2011) revised *Rhipidomys* from Eastern Brazil and showed that these samples previously assigned by Tribe (1996) to *Rhipidomys macrurus* clustered with samples from Tocantins, Bahia and Minas Gerais, that apparently belonged to the same species and accordingly named all of them as *R. macrurus*.

Tribe also identified as *macrurus* the specimens from Serra de Ibiapaba, type locality of *R. cearanus* (Thomas 1910), an idea not accepted by later authors. Gurgel-Filho et al. (2015) recognized *R. cearanus* as a valid species based on morphological differences and the geographic distance between their type localities.

Costa (2003: 82) proposed a phylogenetic hypothesis for the genus *Rhipidomys* and recovered a clade composed by *R. macrurus* and *R. aff. macrurus* (*R. aff. macrurus*=*R. caracolensis*; see synonyms in description section above). Later, based on the analysis of samples from Costa (2003) and other samples, Costa et al. (2011: 953), restricted the concept of *macrurus* to samples from Nova Ponte (MG), Serra da Ca-

nastra (MG), Dourados (MS) and Caldas Novas (GO); these samples formed a distinct clade, although not strongly supported.

We recognized in our morphological analysis a group distributed over Minas Gerais, Goiás, Distrito Federal, Mato Grosso do Sul and Paraguay (Fig. 1 and 2) that we called *R. “macrurus”*. We believe this is the same species called *R. macrurus* by Costa et al. (2011) and Tribe (2015). However, *R. macrurus* Gervais, 1855 is not identifiable, since the holotype was not found in the MNHN collections Tribe (2015: 606) and the original description of *R. macrurus* Gervais, 1855 is insufficient. The external characters given, although sufficient to identify the genus, are not conclusive to identify species since there is considerable variability within species. Most key characters that define species of *Rhipidomys* are in the skull, which was not described by the author.

The type locality of *R. macrurus* is stated in Gervais description as Crixas, Goiás. Topotypic specimens have not been collected at this place to help identification of *R. macrurus*. A specimen labeled as a co-type of *Rhipidomys macrurus* Gervais is found in the Natural History Museum of London under number BMNH 49.12.8.4, but we are not sure if this specimen has some value as type material, accordingly to the ICZN, as there is no mention to it in any published material about this taxon. This specimen is damaged, lacking the basicranium, and the provenance in the label is “Bahia, Castelnau”, a vague information making it impossible to evaluate how far this specimen was obtained from the type locality; according to Papavero (1971) and Whitley (1974), Castelnau acted as the French consul in Salvador, Bahia, in 1848, where he may have captured this specimen. Additionally, no other specimens are mentioned in the original description besides the holotype.

Tribe (2015: 606) suggested a neotype for *R. macrurus* should be designated to ensure the stability of usage of this name. To ensure stability of nomenclature we consider that the selected neotype specimen should have the characters mentioned in our Tab. 2 under *R. “macrurus”* and agree with the *R. macrurus* concept of Costa et al. (2011) belonging to the corresponding molecular phylogenetic clade. Tribe (2015) believes that considerable further research is needed to elucidate the status of all the forms included by him in *R. macrurus*.

Diversity and Conservation of *Rhipidomys* in Northeastern Brazil

Species of the genus *Rhipidomys* are commonly associated with more humid habitats and their distribution in the northeast Brazil occurs in coastal environments of the Atlantic Forest and in the interior humid enclaves (Brejos de Altitude and Gallery Forest). Each one of the six northeastern *Rhipidomys* species occupies different enclaves: *R. cariri* at Araripe plateau; *R. baturiteensis* at Baturité plateau; *R. cearanus* at Ibiapaba plateau; *R. bezerrensis* at one site of Borborema plateau; *R. mastacalis* at Atlantic Forest and most of eastern Borborema plateau enclaves; and *R. caracolensis* at Gallery Forests within Cerrado and Caatinga (Fig. 1 and 2).

These patches of moist vegetation are considered as testimonies of a more comprehensive rainforest that united Amazonia and Atlantic Forest (Silveira et al., 2019; Batalha-Filho et al., 2013; Costa, 2003; Vivo and Carmignotto, 2004). Recently, in a study focusing on modeling the distribution of the Northeastern Atlantic Forest during the Pleistocene, Silveira et al. (2019) defined three biogeographic regions: the Araripe and Pernambuco/Paraíba enclaves; the northernmost North Ceará enclaves (Ibiapaba and Baturité Plateau); and the southernmost Chapada Diamantina enclaves. In their models, the enclaves of the northern Ceará would have a high degree of isolation during the last glacial cycle modeled and that isolation should be consistent in most other preceding glacial cycles (Silveira et al., 2019, 73). On the other hand, the Araripe and Pernambuco/Paraíba enclaves exhibited a dynamic history of connectivity among them, with high connectivity during the LGM and isolation in other periods. This connectivity could explain the closer relationship between *R. bezerrensis* and *R. cariri* in our phylogenetic hypothesis. These fluctuations in forest connectivity may have driven the diversification of *Rhipidomys* species, making it difficult for their populations to spread among enclaves. At least two events of connectivity must have occurred for *Rhipidomys* species, as

can be seen by the two different lineages in this area (*R. bezerrensis* + *R. cariri*) and *R. mastacalis*. Therefore, the preservation of these enclaves is crucial for the conservation of endemic species of *Rhipidomys* that inhabit them, but also for the conservation of the evolutionary and biogeographic processes involved on the history of this biota, that still need to be told. 📄

References

- Ab'Sáber A., 2003. Os domínios de natureza no Brasil. Potencialidades paisagísticas, Ateliê, Cotia. [in Portuguese]
- Ahrens D., Fujisawa T., Krammer H.J., Eberle J., Fabrizi S., Vogler A.P., 2016. Rarity and incomplete sampling in DNA-based species delimitation. *Syst. Biol.* 65: 478–494. doi:10.1093/sysbio/syw002
- Allen J.A., 1916. New mammals collected on the Roosevelt Brazilian Expedition. *Bull. Am. Museum Nat. Hist.* 35: 523–530.
- Andrade-Lima D., 1966. Esboço fitocológico de alguns “brejos” de Pernambuco. *Bol. Técnico Inst. Pesq. Agron. Pernamb.* 8: 3–9. [in Portuguese]
- Andrade-Lima D., 1982. Present-day forest refuges in northeastern Brazil. In: Prance G.T. (Ed.) *Biological Diversification in the Tropics*. Columbia University Press, New York, NY. 245–251.
- Andrades-Miranda J., Oliveira L.F.B., Lima-Rosa C.A.C., Sana D.A., Nunes A.P., Matvevi M.S., 2002. Genetic studies in representatives of genus *Rhipidomys* (Rodentia, Sigmodontinae) from Brazil. *Acta Theriol.* 47: 125–135.
- Anisimova M., Gil M., Dufayard J.F., Dessimoz C., Gascuel O., 2011. Survey of branch support methods demonstrates accuracy, power, and robustness of fast likelihood-based approximation schemes. *Syst. Biol.* 60(5): 685–699. doi:10.1093/sysbio/syr041
- Batalha-Filho H., Fjeldså J., Fabre P.H., Miyaki C.Y., 2013. Connections between the Atlantic and Amazonian forest avifauna represent distinct historical events. *J. Ornithol.* 154(1): 41–50. doi:10.1007/s10336-012-0866-7
- Brandt R.S., Pessoa L.M., 1994. Intrapopulacional variability in cranial character of *Oryzomys subflavus*. *Zool. Anz.* 233: 45–55.
- Brasil, Ministério do Meio Ambiente. Portaria MMA 463 de 18 de dezembro de 2018. DOU nº243 de 19 de dezembro de 2018. [in Portuguese]
- Brito J.M., Tinoco N., Chávez D., Moreno-Cárdenas P., Batallas D., Ojala-Barbour R., 2017. New species of arboreal rat of the genus *Rhipidomys* (Cricetidae, Sigmodontinae) from Sangay National Park, Ecuador. *Neotrop. Biodivers.* 3(1): 65–79. doi:10.1080/23766808.2017.1292755
- Burgin C.J., Colella J.P., Kahn P.L., Upham N.S., 2018. How many species of mammals are there? *J. Mammal.* 99(1): 1–14. doi:10.1093/jmammal/gyx147
- Cabrera A., 1961. Catálogo de los mamíferos de América del Sur. *Rev. del Mus. Argentino Ciencias Nat.* “Bernardino Rivadavia” 4: 309–732. [in Spanish]
- Carleton M.D., Musser G.G., 1989. Systematic studies of oryzomyine rodents (Muridae, Sigmodontinae): a synopsis of *Microrozomys*. *Bull. Am. Museum Nat. Hist.* 191: 1–83.
- Costa L.P., 2003. The historical bridge between the Amazon and the Atlantic Forest of Brazil: a study of molecular phylogeography with small mammals. *J. Biogeogr.* 30: 71–86.
- Costa B.M.A., 2007. Sistemática de *Rhipidomys* (Mammalia: Rodentia) do leste do Brasil. M.Sc. Thesis, Universidade Federal do Espírito Santo, Espírito Santo-ES. [in Portuguese]
- Costa B.M.A., Geise L., Pereira L.G., Costa L.P., 2011. Phylogeography of *Rhipidomys* (Rodentia: Cricetidae: Sigmodontinae) and description of two new species from southeastern Brazil. *J. Mammal.* 92(5): 945–962. doi:10.1644/10-MAMM-A-249.1
- Cracraft J., 1983. Cladistic Analysis and Vicariance Biogeography: Evolutionary biology gains a new dimension from the reconstruction of systematic and biogeographic patterns. *Am. Sci.* 71: 273–281.
- Dal Vechio F., Teixeira M., Recoder R.S., Rodrigues M.T., Zaher H., 2016. A herpetofauna do Parque Nacional da Serra das Confusões, Piauí, Brasil, com uma lista regional para uma área ecológica entre o Cerrado e a Caatinga. *Biota Neotrop.* 16(3): e20150105. doi:10.1590/1676-0611-BN-2015-0105
- Dayrat B., 2005. Towards integrative taxonomy. *Biol. J. Linn. Soc.* 85: 407–415.
- De la Sancha N.U., D'Elia G.D., Tribe C.J., Perez P.E., Valdez L., Pine R.H., 2011. *Rhipidomys* (Rodentia, Cricetidae) from Paraguay: noteworthy new records and identity of the Paraguayan species. *Mammalia* 75(3): 269–276. doi:10.1515/mamm.2011.022
- de Sousa M.A.N., 2005. Pequenos mamíferos (Didelphimorphia, Didelphidae e Rodentia, Sigmodontinae) de algumas áreas da Caatinga, Cerrado, Mata Atlântica e Brejo de Altitude do Brasil: Considerações citogenéticas e geográficas. M.Sc. thesis, Instituto de Biociências, Universidade de São Paulo, São Paulo-SP. [in Portuguese]
- de Sousa M.A.N., Langguth A., Gimenez E.D.A., 2004. Mamíferos dos Brejos de Altitude Paraiba e Pernambuco. In: Porto C.P.K., Cabral J.J.P., Tabarelli M. (Eds.) *Brejos de Altitude Em Pernambuco e Paraiba: História Natural, Ecologia e Conservação*. Ministério do Meio Ambiente – Série Biodiversidade 9, Brasília. 229–254. [in Portuguese]
- Frost D.R., Kluge A.G.D., Hillis M., 1992. Species in contemporary herpetology: comments on phylogenetic inference and taxonomy. *Herpetologica* Rev. 23: 46–54.
- Gervais P., 1855. Cinquième mémoire. Énumération des principaux espèces de mammifères. In: Gervais P. (Ed.) *Mammifères 7e. Partie, Zoologie*. In: de Castelnau F. (Ed.) *Annales nouveaux ou rares recueillis pendant l'expédition dans les parties centrales de l'Amérique du Sud, de Rio de Janeiro à Lima, et de Lima au Pará; exécutée par ordre du gouvernement français pendant les années 1843 à 1847, sous la direction du comte Francis de Castelnau*. 107–116. [in French]
- Gregorin R., Carmignotto A.P., Percequillo A.R., 2008. Quirópteros do Parque Nacional da Serra das Confusões, Piauí, nordeste do Brasil. *Chiropt. Neotrop.* 14(1): 326–383. [in Portuguese]
- Guindon S., Gascuel O., 2003. A Simple, Fast, and Accurate Algorithm to Estimate Large Phylogenies. *Syst. Biol.* 52(5): 696–704. doi:10.1080/10635150390235520
- Guindon S., Dufayard J.F., Lefort V., Anisimova M., Hordijk W., Gascuel O., 2010. New algorithms and methods to estimate maximum-likelihood phylogenies: assessing the performance of PhyML 3.0. *Syst. Biol.* 59(3): 307–321. doi:10.1093/sysbio/syq010
- Gurgel-Filho N.M., Feijó A., Langguth A., 2015. Pequenos Mamíferos do Ceará (Marsupiais, Morcegos e Roedores Sigmodontineos) com discussão taxonômica de algumas espécies. *Rev. Nord. Biol.* 23(2): 3–150. doi:10.1017/CBO9781107415324.004 [in Portuguese]
- Gyldenstolpe N., 1932. A manual of Neotropical Sigmodont rodents. *K. Sven. Vetenskapssakad. Handl.* 11(3): 1–164.
- Hair J.F., Anderson R.E.,athan R.L., Black W.C., 2007. Análise multivariada de dados. Editora Artmed, São Paulo. [in Portuguese]
- Hair J.F., Black W.C., Babin B.J., Anderson R.E.,athan R.L., 2009. Análise Multivariada de Dados. Editora Artmed, São Paulo. [in Portuguese]
- Hall T.A., 1999. BioEdit: a user-friendly biological sequence alignment editor and analysis program for Windows 95/98/NT. *Nucleic Acids Symp.* 41: 95–98. doi:10.1039/c7qj00394c
- Hammer Ø., Harper D.A.T., Ryan P.D., 2001. PAST: Paleontological statistics software package for education and data analysis. *Palaeontol. Electron.* 4(1): 1–9. doi:10.1016/j.bcp.2008.05.025
- Hershkovitz P., 1962. Evolution of Neotropical Cricetine Rodents (Muridae) - With Special reference to the Phyllotine group. *Fieldiana Zool.* 46(1): 1–524.
- Keane T.M., Creevey C.J., Pentony M.M., Naughton T.J., McInerney J.O., 2006. Assessment of methods for amino acid matrix selection and their use on empirical data shows that ad hoc assumptions for choice of matrix are not justified. *BMC Evol. Biol.* 6: 1–17. doi:10.1186/1471-2148-6-29
- Librado P., Rozas J., 2009. DnaSP v5: A software for comprehensive analysis of DNA polymorphism data. *Bioinformatics* 25(11): 1451–1452. doi:10.1093/bioinformatics/btp187
- Miller M.A., Pfeiffer W., Schwartz T., 2010. Creating the CIPRES Science Gateway for inference of large phylogenetic trees. 2010 *Gatew. Comput. Environ. Work. GCE* 2010. doi:10.1109/GCE.2010.5676129
- Musser G.G., 1968. A Systematic Study of the Mexican and Guatemalan Gray Squirrel, *Sciurus aureogaster* F. Cuvier (Rodentia: Sciuridae). *Misc. Publ. Museum Zool. Univ. Michigan* 137: 1–112.
- Musser G.G., Carleton M.D., 1993. Family Muridae. In: Wilson D.E., Reeder D.M. (Eds.) *Mammal Species of the World: A Taxonomic and Geographic Reference*. Smithsonian University Press, Washington, DC. 501–755.
- Musser G.G., Carleton M. D., 2005. Superfamily Muroidea. In Wilson D.E., Reeder D.M. (Eds.) *Mammal Species of the World. A Taxonomic and Geographic reference*. 3rd ed. The Johns Hopkins University Press, Baltimore. 894–1531.
- Oliveira J.A., 1992. Estrutura da variação craniana em populações de *Bolomys lasiurus* (Lund, 1841) (Rodentia: Cricetidae) do Nordeste do Brasil. M.Sc. Thesis, Universidade Federal do Rio de Janeiro, Rio de Janeiro-RJ. [in Portuguese]
- Pacheco V., Patton J.L., D'Elia G., 2015. Tribe Thomasomyini Steadman and Ray, 1982. In: Patton J.L., Pardiñas U.F.J., D'Elia G. (Eds.) *Mammals of South America – Vol. 2*. University of Chicago Press. 571–681.
- Paixão V. dos S., Suárez P., Oliveira da Silva W., Geise L., Ferguson-Smith M.A., O'Brien P.C.M., Mendes-Oliveira A.C., Rossi R.V., Pieczarka J.C., Nagamachi C.Y., 2021. Comparative genomic mapping reveals mechanisms of chromosome diversification in *Rhipidomys* species (Rodentia, Thomasomyini) and syntenic relationship between species of Sigmodontinae. *PLoS One* 16: e0258474. doi:10.1371/journal.pone.0258474
- Papavero N., 1971. Essays on the History of Neotropical Dipterozoology: with special reference to collectors: 1750-1905: Vol. I, Museu de Zoologia, BR.
- Patton J.L., Da Silva M.N.F., Malcolm J.R., 2000. Mammals of the Rio Juruá and the Evolutionary and Ecological Diversification of Amazonia. *Bull. Am. Museum Nat. Hist.* 244(244): 1. doi:10.1206/0003-0090(2000)244<0001:MOTRJA>2.0.CO;2
- Percequillo A.R., 1998. Sistemática de *Oryzomys* Baird, 1858 do Leste do Brasil (Muroidea, Sigmodontinae). M.Sc. thesis, Universidade de São Paulo, São Paulo-SP. [in Portuguese]
- Pôrto K.C., Cabral J.J.P., Tabarelli M., 2004. Brejos de Altitude em Pernambuco e Paraíba. *História Natural, Ecologia e Conservação*. Ministério do Meio Ambiente, Brasília. [in Portuguese]
- Rambaut A., 2016. FigTree 1.4.3. Available from <http://tree.bio.ed.ac.uk/software/figtree> [21 May 2018]
- Rambaut A., Drummond A. J., Suchard M., 2014. Tracer v. 1.6. Available from: <http://beast.bio.ed.ac.uk/Tracer> [09 June 2018]
- Reig O., 1977. A proposed unified nomenclature for the enamelled components of the molar teeth of the Cricetidae (Rodentia). *J. Zool.* 181: 227–241. doi:10.1111/j.1469-7998.1977.tb03238.x
- Reis S.F., 1988. Morfometria e estatística multivariada em biologia evolutiva. *Rev. Bras. Zool.* 4(4): 571–580. [in Portuguese]
- Rocha R.G., Ferreira E., Costa B.M.A., Martins I.C.M., Leite Y.L.R., Costa L.P., Fonseca C., 2011. Small mammals of the mid-Araguari River in central Brazil, with the description of a new species of climbing rat. *Zootaxa*. 2789: 1–34.
- Sikes R.S., 2016. 2016 Guidelines of the American Society of Mammalogists for the use of wild mammals in research and education. *J. Mammal.* 97(3): 663–688. doi:10.1093/jmammal/gyw078
- Silveira M.H.B., Mascarenhas R., Cardoso D., Batalha-Filho H., 2019. Pleistocene climatic instability drove the historical distribution of forest islands in the northeastern Brazilian Atlantic Forest. *Palaeogeogr. Palaeoclimatol. Palaeoecol.* 527: 67–76. doi:10.1016/j.palaeo.2019.04.028
- Smith M.F., Patton J.L., 1993. The diversification of South American murid rodents: evidence from mitochondrial DNA sequence data for akodontine tribe. *Biol. J. Linn. Soc.* 50: 149–177. doi:10.1111/j.1095-8312.1993.tb00924.x
- Steppan S.J., 1995. Revision of the Tribe Phyllotini (Rodentia: Sigmodontinae), with a Phylogenetic Hypothesis for the Sigmodontinae. *Fieldiana Zool.* 80: 1–132.
- Tabarelli M., Santos A.M.M., 2004. Uma breve descrição sobre a história natural dos brejos nordestinos. In: Porto C.P.K., Cabral J.J.P., Tabarelli M. (Eds.) *Brejos de Altitude Em Pernambuco e Paraíba: História Natural, Ecologia e Conservação*. Ministério do Meio Ambiente – Série Biodiversidade 9, Brasília. 324. [in Portuguese]
- Tate G.H.H., 1932. The taxonomic history of the south and central american oryzomyine genera of rodents (excluding *Oryzomys*): *Nesoryzomys*, *Zygodontomys*, *Chilomys*, *Delomys*, *Phaenomys*, *Rhagomys*, *Rhipidomys*, *Nyctomys*, *Oecomys*, *Thomasomys*, *Inomys*, *Apomys*, *Neacomys* and *Scolomys*. *Am. Museum Novit.* 581: 1–28.
- The GIMP Development Team, 2019. GIMP. Available from <https://www.gimp.org>
- Thomas O., 1886. XXIV – Description of a new Brazilian species of *Hesperomys*. *Ann. Mag. Nat. Hist.* 17(99): 250–251. doi:10.1080/00222938609460140
- Thomas O., 1906. LXVIII – Notes on South-American Rodents. *Ann. Mag. Nat. Hist.* 18(108): 442–448. doi:10.1080/00222930608562646
- Thomas O., 1910. LVI – On mammals collected in Ceará, N. E. Brazil, by Fräulein Dr. Sneath. *Ann. Mag. Nat. Hist.* 6: 500–503.

- Thomazini N.B., 2013. Correlação entre estrutura cariotípica e filogenia molecular em *Rhipidomys* (Cricetidae, Rodentia) do leste do Brasil. M.Sc. thesis, Universidade Federal do Espírito Santo, Vitória-ES. [in Portuguese]
- Tribe C.J., 1996. The Neotropical rodent genus *Rhipidomys* (Cricetidae, Sigmodontinae) – a taxonomic revision. Ph.D. Thesis, University College London, London, UK.
- Tribe C., 2005. A new species of *Rhipidomys* (rodentia, muroidea) from north-eastern Brazil. *Aquivos do Mus. Nac. Rio Janeiro* 63(1): 131–146.
- Tribe C.J., 2015. Genus *Rhipidomys* Tschudi, 184. In: Patton J.L., Pardiñas U.F.J., D’Elia G. (Eds.) *Mammals of South America - Vol. 2*. University of Chicago Press, Chicago, IL, 583–617.
- Vanzolini P.E., 1993. Métodos estatísticos elementares em sistemática zoológica. Hucitec, São Paulo. [in Portuguese]
- Vitecek S., Kučinić M., Previšić A., Živić I., Stojanović K., Keresztes L., Bálint M., Hoppeler F., Waringer J., Graf W., Pauls S.U., 2017. Integrative taxonomy by molecular species delimitation: multi-locus data corroborate a new species of Balkan Drusinae micro-endemics. *BMC Evol. Biol.* 17: 1–18. doi:10.1186/s12862-017-0972-5
- Vivo M., Carmignotto A., 2004. Holocene vegetation change and the mammal faunas of South America and Africa. *J. Biogeogr.* 31: 943–957. doi:10.1111/j.1365-2699.2004.01068.x
- Voss R.S., 1988. Systematics and ecology of Ichthyomyine rodents (Muroidea): patterns of morphological evolution in a small adaptive radiation. *Bull. Am. Museum Nat. Hist.* 188: 259–493.
- Voss R.S., 1991. An Introduction To the Neotropical Muroid Rodent Genus *Zygodontomys*. *Bull. Am. Museum Nat. Hist. Am.* 210: 1-113. <http://hdl.handle.net/2246/905>
- Voss R.S., 1993. A revision of the Brazilian muroid rodent genus *Delomys* with remarks on “Thomasomyine” Characters. *Am. Museum Novit.* 3073: 1–44.
- Voss R.S., Carleton M.D., 1993. A New Genus for *Hesperomys molitor* Winge and *Holochilus magnus* Hershkovitz (Mammalia, Muridae) with an Analysis of Its Phylogenetic Relationships. *Am. Museum Novit.* 3085: 1–39.
- Whitley G.P., 1974. Laporte, François Louis Nompard de Caumont (1810–1880). *Australian Dictionary of Biography*, National Centre of Biography, Australian National University <http://adb.anu.edu.au/biography/laporte-francois-louis-nompard-de-caumont-3993/text6315> [25 November 2020]
- Zhang J., Kapli P., Pavlidis P., Stamatakis A., 2013. A general species delimitation method with applications to phylogenetic placements. *Bioinformatics* 29: 2869–2876. doi:10.1093/bioinformatics/btt499

Associate Editor: P. Colangelo

Supplemental information

Additional Supplemental Information may be found in the online version of this article:

Figure S1 Bayesian Inference phylogeny.

Figure S2 Maximum Likelihood phylogeny.

Figure S3 Skulls for the 13 morphological groups.

S4 Poisson Tree Process model (bPTP) results.

Table S5 Root values for the variables of the Canonical Analyses.

Figure S6 Example of differential wear of molars used for age class determination.

Figure S7 PCA biplot.

Table S8 perMANOVA PAST results.

Appendix A

List of species and specimens analyzed with Genbank, Museum or Field Number, haplotype code and locality name. NGO=North Goiás; WTO=West Tocantins; SPI=Southern Piauí; WBA=Western Bahia; NMG=Northern Minas Gerais.

Accession No.	Voucher ID	Site	State	Country	Species	Haplotype
KY366345	QCAZ15214	Morona Santiago		Ecuador	<i>Rhipidomys albujaei</i>	H1
	ARP152	Caracol	Piauí	Brazil	Samples from NGO, WTO, SPI, WBA, NMG	H10
	LGA463	PN Grande Sertões Veredas	Minas Gerais	Brazil	Samples from NGO, WTO, SPI, WBA, NMG	H11
	LGA923	Jalapão	Tocantins	Brazil	Samples from NGO, WTO, SPI, WBA, NMG	H12
HM594666		Chapada do Araripe	Ceará	Brazil	<i>Rhipidomys cariri</i>	H13
HM594661		Altamira	Pará	Brazil	<i>Rhipidomys emiliae</i>	H14
AF108682		Altamira	Pará	Brazil	<i>Rhipidomys emiliae</i>	H14
HM594657		Parauapebas	Pará	Brazil	<i>Rhipidomys emiliae</i>	H15
HM594636		Carajás	Pará	Brazil	<i>Rhipidomys emiliae</i>	H15
HM594635		Carajás	Pará	Brazil	<i>Rhipidomys emiliae</i>	H15
HM594634		Carajás	Pará	Brazil	<i>Rhipidomys emiliae</i>	H15
HM594656		Vila Rica	Mato Grosso	Brazil	<i>Rhipidomys emiliae</i>	H16
HM594641		Ribeirão Cascalheira	Mato Grosso	Brazil	<i>Rhipidomys emiliae</i>	H16
HM594642		Ribeirão Cascalheira	Mato Grosso	Brazil	<i>Rhipidomys emiliae</i>	H17
HM594639		Barra do Garças	Mato Grosso	Brazil	<i>Rhipidomys emiliae</i>	H17
HM594638		Barra do Garças	Mato Grosso	Brazil	<i>Rhipidomys emiliae</i>	H17
HM594637		Barra do Garças	Mato Grosso	Brazil	<i>Rhipidomys emiliae</i>	H17
HM594640		Barra do Garças	Mato Grosso	Brazil	<i>Rhipidomys emiliae</i>	H18
HM622065		Rio Juruá	Acre	Brazil	<i>Rhipidomys gardneri</i>	H19
HQ634182		Cusco		Peru	<i>Rhipidomys gardneri</i>	H19
KY366343	DMMECN3719	Morona Santiago		Ecuador	<i>Rhipidomys albujaei</i>	H2
KY366342	DMMECN3790	Morona Santiago		Ecuador	<i>Rhipidomys albujaei</i>	H2
HM594673		Cusco		Peru	<i>Rhipidomys gardneri</i>	H20
U03550		Madre de Dios		Peru	<i>Rhipidomys gardneri</i>	H21
HM594633		Peixe	Tocantins	Brazil	<i>Rhipidomys ipukensis</i>	H22
HM594628		Lagoa da Confusão	Tocantins	Brazil	<i>Rhipidomys ipukensis</i>	H22
HM594632		Lagoa da Confusão	Tocantins	Brazil	<i>Rhipidomys ipukensis</i>	H23
HM594631		Lagoa da Confusão	Tocantins	Brazil	<i>Rhipidomys ipukensis</i>	H23
HM594630		Lagoa da Confusão	Tocantins	Brazil	<i>Rhipidomys ipukensis</i>	H23
HM594629		Pium	Tocantins	Brazil	<i>Rhipidomys ipukensis</i>	H23
HM594627		Lagoa da Confusão	Tocantins	Brazil	<i>Rhipidomys ipukensis</i>	H23
HM594658		Guarapimirim	Rio de Janeiro	Brazil	<i>Rhipidomys itoan</i>	H24
HM594654		Ilha Grande	São Paulo	Brazil	<i>Rhipidomys itoan</i>	H24
HM594649		Pilar do Sul	São Paulo	Brazil	<i>Rhipidomys itoan</i>	H25
HM594648		Boraceia	São Paulo	Brazil	<i>Rhipidomys itoan</i>	H26
AF108683		Boraceia	São Paulo	Brazil	<i>Rhipidomys itoan</i>	H26
HQ634183		Aripuanã	Mato Grosso	Brazil	<i>Rhipidomys leucodactylus</i>	H27
HM594659		Aripuanã	Mato Grosso	Brazil	<i>Rhipidomys leucodactylus</i>	H27
HM622064		Juruá	Amazonas	Brazil	<i>Rhipidomys leucodactylus</i>	H28
HM594668		Juruá	Amazonas	Brazil	<i>Rhipidomys leucodactylus</i>	H29
KY366344	MEPN12196	Morona Santiago		Ecuador	<i>Rhipidomys albujaei</i>	H3
HM594674		Cerro de la Neblina		Venezuela	<i>Rhipidomys macconnelli</i>	H30
AF108681		Cerro de la Neblina		Venezuela	<i>Rhipidomys macconnelli</i>	H31
AY275130		Cerro de la Neblina		Venezuela	<i>Rhipidomys macconnelli</i>	H32
HM622062		Caldas Novas	Goiás	Brazil	<i>Rhipidomys macrurus</i>	H33
FJ3610741		Ipameri	Goiás	Brazil	<i>Rhipidomys macrurus</i>	H33
HQ634181		Nova Ponte	Minas Gerais	Brazil	<i>Rhipidomys macrurus</i>	H34
HM594646		Nova Ponte	Minas Gerais	Brazil	<i>Rhipidomys macrurus</i>	H34
HQ634180		Canindeyu		Paraguay	<i>Rhipidomys macrurus</i>	H35
HM594650		Serra da Canastra	Minas Gerais	Brazil	<i>Rhipidomys macrurus</i>	H36
HM594647		Dourados	Mato Grosso do Sul	Brazil	<i>Rhipidomys macrurus</i>	H37
HM594645		Nova Ponte	Minas Gerais	Brazil	<i>Rhipidomys macrurus</i>	H38
HM622063		Uruçuca	Bahia	Brazil	<i>Rhipidomys mastacalis</i>	H39
HM594652		Una	Bahia	Brazil	<i>Rhipidomys mastacalis</i>	H39
	FO03	Bezerros	Pernambuco	Brazil	Samples from Bezerros	H4
	FO15	Bezerros	Pernambuco	Brazil	Samples from Bezerros	H4
	FO18	Bezerros	Pernambuco	Brazil	Samples from Bezerros	H4
	FO23	Bezerros	Pernambuco	Brazil	Samples from Bezerros	H4
	FO34	Bezerros	Pernambuco	Brazil	Samples from Bezerros	H4

Appendix 1 (continued) List of species and specimens analyzed with Genbank, Museum or Field Number, haplotype code and locality name. NGO=North Goiás; WTO=West Tocantins; SPI=Southern Piauí; WBA=Western Bahia; NMG=Northern Minas Gerais.

Accession No.	Voucher ID	Site	State	Country	Species	Haplotype
HM594653		Nova Viçosa	Bahia	Brazil	<i>Rhipidomys mastacalis</i>	H40
HM594651		Marileria	Minas Gerais	Brazil	<i>Rhipidomys mastacalis</i>	H41
HM594644		Turmalina	Mato Grosso	Brazil	<i>Rhipidomys mastacalis</i>	H42
HM594643		São Gonçalo do Rio Preto	Minas Gerais	Brazil	<i>Rhipidomys mastacalis</i>	H43
AF108684		Linhares	Espírito Santo	Brazil	<i>Rhipidomys mastacalis</i>	H44
HM594655		Una	Bahia	Brazil	<i>Rhipidomys mastacalis</i>	H45
HM594665		Pic Metechau		French Guiana	<i>Rhipidomys nitela</i>	H46
EU579475		Baramita		Guiana	<i>Rhipidomys nitela</i>	H47
HM594664		Les Nourague		French Guiana	<i>Rhipidomys nitela</i>	H48
HM594663		Parque do Caraça	Minas Gerais	Brazil	<i>Rhipidomys tribei</i>	H49
HM594662		Fervedouro	Minas Gerais	Brazil	<i>Rhipidomys tribei</i>	H49
HM594672		Minaçu	Goiás	Brazil	Samples from NGO, WTO, SPI, WBA, NMG	H5
HQ634184		Cerro de la Neblina		Venezuela	<i>Rhipidomys wetzeli</i>	H50
HM594660		Cerro de la Neblina		Venezuela	<i>Rhipidomys wetzeli</i>	H51
AF108680		Cerro de la Neblina		Venezuela	<i>Rhipidomys wetzeli</i>	H51
HM594671		Andaraí	Bahia	Brazil	Samples from NGO, WTO, SPI, WBA, NMG	H6
HM594670		Caratinga	Minas Gerais	Brazil	Samples from NGO, WTO, SPI, WBA, NMG	H7
M594667		Coronel Murta	Minas Gerais	Brazil	Samples from NGO, WTO, SPI, WBA, NMG	H7
HM594669		Paraná	Tocantins	Brazil	Samples from NGO, WTO, SPI, WBA, NMG	H8
	ARP151	Caracol	Piauí	Brazil	Samples from NGO, WTO, SPI, WBA, NMG	H9
	TG21	Guadalupe	Piauí	Brazil	Samples from NGO, WTO, SPI, WBA, NMG	H52
	MN36449	Colinas do Sul	Goiás	Brazil	Samples from NGO, WTO, SPI, WBA, NMG	H53

Appendix B

Specimens of *Rhipidomys* examined, by species.

Brazilian States are given in bold uppercase, followed by a number in bold that correspond to specific localities shown in maps (Fig. 1 and 2) and listed in the gazetteer (Appendix C). Specimen identification numbers, museum numbers or collector numbers, follow in parentheses. Holotypes examined are marked with an asterisk *. For museum acronyms and other abbreviations, see text.

Rhipidomys leucodactylus.— **AMAPÁ: 11** (MPEG 2508); **RONDÔNIA: 143** (UFPP 1258-1260); no location (UFPP 2696).

Rhipidomys "macrurus" (sensu Tribe, 2015).— **DISTRITO FEDERAL: 41** (MN 21378, 21379); **65** (BAC 10); **GOIÁS: 50** (MN 4305, 4323); **53** (MZUSP 4005, 4006, 4008); **54** (MZUSP 3991, 3993, 3994, 4010, 4015, 4030); **55** (OT7657, OT50701, OT76571); **MINAS GERAIS: 68** (PUC-MG 152); **69** (UFMG 1776); **70** (UFMG 1775); **71** Loc 2 (RG 14,16); **72** (FV 32, 47, 49); **74** (MZUSP 1979, 3992, 4004, 4011, 4021, 4028); **75** (UFMG 1703); **77** Loc 1 (UFMG 2943); Loc 2 (UFMG 1936, 2944); Loc 3 (UFPP 3774).

Rhipidomys baturiteensis.— **CEARÁ: 34** Loc 1 (MN 30011); Loc 2 (MN 17373, 17441, 17444, 30010); Loc 3 (MN 17440, 17442, 17443, 17446, 30005–30009); Loc 4 (MN 17431, 17445); Loc 5 (MN 17428*); Loc 6 (MN 30011); Loc 7 (MRT 78).

Rhipidomys mastacalis.— **ALAGOAS: 2** (BC 33); **3** (MN 17450); **4** (UFPE 1557); **BAHIA: 17** (MN 22277); **18** Loc 1 (MN 17300-17302, 17304-17306); Loc 2 (MN 17376, 17303, 61650); **20** Loc 1 (MN 10721, 10786, 10787, 10862, 10952, 11214, 30019, 30020, 9127, 9128, 9131, 9453, 9473, 9506, 9606, 9657); Loc 2 (MN 11651); **21** (MN 17375, 17447); **22** Loc 1 (UFMG 2041); Loc 2 (UFMG 20530, 2933); Loc 3 (UFMG 2236); Loc 4 (UFPP 425, 426); **23** (CC 27, 30); **24** (MN 48025); **25** Loc 1 (SLF 103); Loc 2 (MN 48004-48006); **26** (MN 61650); **27** (MN 29634, 29782, 29786, 29789, 29807, 29811, 29818); **ESPIRITO SANTO: 44** (MN 34492); **45** Loc 1 (YL 433); Loc 2 (YL 378, 435, 422, 427); **46** (YL 326); **MINAS GERAIS: 78** (UFMG 1649, 1657); **79** Loc 1 (MCN-M PUC 574, 582, 599, 708, 712, 717); Loc 2 (PUC-MG 549); Loc 3 (MCN-M PUC 857, 880); **80** Loc 1 (UFMG 1605, 1606, 1612); Loc 2 (MCN-M PUC 49); **82** (MN 30033; ZMUC.L. 16*); **83**. (MCN-M PUC 857); **84** (UFMG 2931, 1110, 1122); **85** (UFMG 2925-2929); **86** (UFMG 2930); **87** (UFMG 1456, 1460, 1461); **88** (UFMG 1450); **89** (CO 85). **PARAÍBA: 122** (BC 223); **123** (JFL 27–30); **PERNAMBUCO: 124** Loc 1 (UFPP 946, 947, 2569, 2572–2574, 2576, 2578, 2579, 2581–2586, 2588–2592, 2594, 2613, 2616, 2645, 2648, 4386); Loc 2 (MN17358, 17360); Loc 3 (MN 12375, 12380, 17354, 17364, 17367); Loc 4 (MZUSP 24041, UFPP 2572, 2573, MN 12386, 12391, 12508, 12512, 12514, 12515, 12517, 12520, 12521, 17363, 17368, 17381); Loc 5 (MN 12373, 12507, 12510, 12511, 12518, 12519, 17448); Loc 6 (MN 12365, 17346); **125** (UFPP 4500, 4816, 4826, FO 88); **126** (MN 12500); **127** (ALN 109–112, 129, 133); **128** Loc 1

(UFPE 1565), Loc 2 (CMB 6, 15), Loc 3 (CMB 14); **129** (UFPE 1431, 1432); **130** (CMB 9, 10).

Rhipidomys tribei.— **MINAS GERAIS: 90** Loc 1 (UFMG 1937, 1945*[HM594663]); Loc 2 (UFMG 1403–1406); **91** (UFMG 1893); **92** (UFMG 1190).

Samples from North Goiás, West Tocantins, Southern Piauí, Western Bahia and Northern Minas Gerais.— **BAHIA: 15** (UFMG 2935–2938); **13** (MN 4168, 4174); **14** (MN 41420); **PIAÚ: 133** (MzUSP 35682, 35683, 35684, 35685, 35686, 35687*, 35688, 35689, 35690, 35691, 35692); **MINAS GERAIS: 93** (UFMG 2461); **94** (UFMG 2934); **95** (MN 34408, 34409); **97** (MC-PUC 1005); **98** (MzUSP 35435, 35436).

Rhipidomys cariri.— **CEARÁ: 35** Loc 1 (MN 1530, 17313, UFMG 2940, 2941); Loc 2 (MN 10170*, 17299, 17929); Loc 3 (MN 17348, 17349); Loc 4 (MN 30013); Loc 5 (MN 17378, 17417, 17418, 17420–17423); Loc 6 (MN 17379); Loc 7 (MN 30012). **PERNAMBUCO: 131** (UFPP 4820).

Samples from Bezerros.— **PERNAMBUCO: 132** (UFPP 4057, 4058*, 4059, 4060, 4061, 6563).

Rhipidomys cearanus.— **CEARÁ: 30** Loc 1 (MN 12548, 12550); Loc 2 (MN 12395, 12538, 12557); Loc 3 (MN 12527, 12530); Loc 4 (MN 10170, 12534, 12536, 17410); Loc 5 (MRT 3883, MN 12529, 12535); Loc 6 (MN 12377, 12394, 12543); Loc 7 (MN 12389, 12392, 12397, 12400, 12498); Loc 8 (MN 12399, 17402, 17404); Loc 9 (MN 12497, 12540, 17406); Loc 10 (MN 12524); Loc 11 (MN 12555). **37** Loc 1 (MN 17316); Loc 2 (MN 17424, 17427, 17437); Loc 3 (MN 12531, 12564, 17307, 17308, 17311, 17315, 17433, 17438); Loc 4 (MN 12533, 17317); Loc 5 (MN 17310); Loc 6 (MN 17318); Loc 7 (MN 17429); Loc 8 (MN 17432); Loc 9 (MN 17435). **36** (BMNH 11.4.25.7*, holotype, picture); **38** (UFPP 4690).

Rhipidomys itoan.— **RIO DE JANEIRO: 140** Loc 1 (MN 24389); **142** (MN 46805, MN 63605); **SÃO PAULO: 149** (MzUSP 29378, 29380, 29381, 10816); **150** (MzUSP 880).

Rhipidomys emiliae.— **MATO GROSSO: 61** (BMNH 81.374-7); **64** (UFMG 2953); **PARÁ: 110** Loc 1 (MzUSP 21316); **111** (MPEG 34002, 34277).

Rhipidomys nitela.— **BRAZIL: AMAZONAS: 10** (MPEG 7209); (BMNH 1. 6.4.81*, holotype, picture);

Appendix C

Gazetteer.

Collecting localities of *Rhipidomys* species in Brazil. Numbers in bold correspond to numbered localities on the map (Fig. 1 and 2) and in the list of specimens examined (Appendix A). Brazilian states are listed in bold uppercase, followed by municipalities in bold lowercase, and by locality names, latitude and longitude, and elevation (when available) in regular case. Localities listed were taken from labels of specimens examined or from the literature (Allen, 1916; Patton et al., 2000; Tribe, 2005; Costa et al., 2011; Rocha et al., 2011; Tribe, 2015). Geographic coordinates are for a general reference, they were not necessarily measured at collecting points, some were taken from specimens labels, from several gazetteers and others are the seat of the municipality.

ACRE

1.– **Cruzeiro do Sul**, Rio Juruá, above Cruzeiro do Sul, 7°38' S, 72°36' W.

ALAGOAS

- 2.– **Murici**, Estação Ecológica de Murici, 9°13' S, 35°53' W;
3.– **Anádia**, Sítio Vale Verde, 9°42' S, 36°18' W;
4.– **Ibateguara**, Usina Serra Grande, Mata de Aquidabã, 9°0' S, 35°52'12" W.

AMAZONAS

- 5.– **Ipixuna**, Condor, left bank Rio Juruá, 6°45' S, 70°51' W;
6.– **Penedo**, right bank Rio Juruá, 6°50' S, 70°45' W;
7.– **Eirunepé**, Rio Juruá, 6°40' S, 69°52' W;
8.– **Altamira**, right bank Rio Juruá, 6°35' S, 68°54' W;
9.– Fazenda Esteio, 80 km NNE of Manaus, and INPA forest reserves, 2°25' S, 59°50' W;
10.– **Manaus**, Manaus-Itacoatiara Road, km 50, 2°40' S, 59°55' W.

AMAPÁ

- 11.– **Mazagão**, Boa Fortuna upper Igarapé Rio Branco 0°33' N, 52°12' W;
12.– Mouth of Rio Branco, Rio Maracá, 0°32' N, 52°12' W.

BAHIA

- 13.– **Barreiras**, 12°8' S, 45°0' W;
14.– **Bom Jesus da Lapa**, 13°15' S, 43°25' W;
15.– **Andaraí**, Fazenda Santa Rita, 8 km E de Andaraí, 12°48'6" S, 41°5'41" W;
16.– **Formosa do Rio Preto**, São Marcelo, 11°2' S, 45°32' W;
17.– **São Felipe**, 12°51' S, 39°6' W;
18.– **Jequié**, Loc 1 = Fazenda Baixa Bonita, 13°51' S, 40°5' W; Loc 2 = Fazenda Baixa da Fartura, 13°51' S, 40°25' W;
19.– Três Braços, 37 km N and 34 km E of Jequié, Fazenda Nova Esperança, 13°32' S, 39°45' W;
20.– **Ihéus**, Loc 1 = 14°49' S, 39°2' W; Loc 2 = Urucutuca, Aritaguá, 14°40' S, 39°7' W; Loc 3 = Campus CEPLAC, 14°46' S, 39°13' W; Loc 4 = Fazenda Santa Maria, 14°42' S, 39°10' W;
21.– **Vitória da Conquista**, Loc 1 = Sítio Cachoeira dos Porcos, Sítio Caititu de Graciano, approx. 14°51' S, 40°51' W; Loc 2 = Sítio Batalha, 14°48' S, 40°54' W;
22.– **Una**, Loc 1 = Fazenda Jueirana, 15°21' S, 39°0' W; Loc 2 = Fazenda Bolandeiras, 10 km S de Una, 15°21' S, 39°0' W; Loc 3 = Companhia Agropecuária Sul da Bahia; Loc 4 = EDJAB, CEPLAC; Loc 5 = Fazenda Unacau, 8 km SE São José, 15°6' S, 39°16' W;
23.– **Canavieiras**, Fazenda Santa Clara, 15°34' S, 39°4' W;
24.– **Prado**, Cumuruxatiba, 17°6' S, 39°10' W [5 m];
25.– **Nova Viçosa**, Loc 1 = Fazenda Elma, 17°58'31" S, 39°33'52" W [33 m]; Loc 2 = Helvécia, Nova Viçosa, 17°48' S, 39°39' W [52 m];
26.– **Jaborandi**, Fazenda Sertão Formoso, 14°29' S, 45°48' W;
27.– **Jussari**, RPPN Serra do Teimoso, 15°9' S, 39°32' W;
28.– **Cairu**, Fazenda Subauma, 13°31' S, 39°2' W;
29.– **Itamari**, Fazenda Alto São Roque, 13°51' S, 39°40' W;
30.– **Uruçuca**, Estação Central de Experimentação de Cacau, 14°35' S, 39°16' W;
31.– Almada, Rio do Braço, 14°40' S, 39°15' W;
32.– **Buerarema**, Ribeirão da Fortuna, 14°58' S, 39°14' W;
33.– **Guaratinga**, Fazenda Vista Bela, 16°36' S, 39°55' W.

CEARÁ

- 34.– **Pacoti**, Loc 1 = Sítio Ladeira, 4°13' S, 38°56' W; Loc 2 = Sítio Ouro, 4°13' S, 38°56' W; Loc 3 = Sítio Santa Rosa Dr. Luiz, 4°13' S, 38°56' W; Loc 4 = Sítio Pirajá, 4°13' S, 38°56' W; Loc 5 = Sítio Cebola, 4°13' S, 38°56' W; Loc 6 = Sítio Ladeira, 4°13' S, 38°56' W; Loc 7 = Sítio Friburgo, 4°13' S, 38°56' W;
35.– **Crato**, Loc 1 = Crato, 7°13' S, 39°27' W; Loc 2 = Sítio Caiano, 7°13' S, 39°27' W; Loc 3 = Sítio Passagem Primeira, 7°13' S, 39°27' W; Loc 4 = Sítio Passagem Segunda, 7°13' S, 39°27' W; Loc 5 = Sítio Belo Horizonte, 7°13' S, 39°27' W; Loc 6 = Sítio Arisco, 7°13' S, 39°27' W; Loc 7 = Sítio Baixa do Maracujá, 7°13' S, 39°27' W;
36.– **São Benedito**, includes at coordinates 4°3' S, 40°53' W the following localities: Loc 1 = Sítio Cigarro; Loc 2 = Sítio Piraguara; Loc 3 = Sítio Macapá; Loc 4 = Sítio Bom Jardim; Loc 5 = Sítio Guaribas do Amaral; Loc 6 = Sítio São José da Boa Vista; Loc 7 = Sítio Barra; Loc 8 = Sítio Cinta da Soledade; Loc 9 = Sítio Alto; Loc 10 = Sítio Buenos Aires; Loc 11 = Sítio Santa Luzia; Loc 12 = São Paulo: on the top of the Serra de Ibiapaba [900 m], 4°3' S, 40°53' W;
37.– **Guaraciaba do Norte**, includes at coordinates 4°10' S, 40°46' W the following localities: Loc 1 = Sítio Mandu; Loc 2 = Sítio Flores; Loc 3 = Sítio Mazagão; Loc 4 = Sítio Cacimba do Meio; Loc 5 = Sítio Riacho Fundo; Loc 6 = Sítio Rua Nova; Loc 7 = Sítio São Tomé; Loc 8 = Sítio Quati; Loc 9 = Sítio Tomé;
38.– **Ipu**, Serra de Ibiapaba, 7 km de Ipu [750 m], 4°16'18" S, 40°44'41" W.

DISTRITO FEDERAL

- 39.– **Planaltina**, Reserva Biológica de Águas Emendadas, 15°33' S, 47°35' W;
40.– Parque Nacional de Brasília (includes Granja do Ipê, Ribeirão Bananal), 15°35' S, 47°54' W;

41.– Brasília, [aprox. 1000 m] (also includes: Fundação Zoobotânica; Jardim Zoológico), approx. 15°47' S, 47°55' W;

42.– **Brasília** Reserva do IBGE, 25 km S of Brasília, approx. 1000 m, 15°58' S, 47°54' W;

43.– Fazenda Água Limpa, 20 km S of Brasília, approx. 1000 m, 15°58' S, 47°57' W.

ESPIRITO SANTO

- 44.– **Linhares**, Fazenda Cupido, approx. 19°10' S, 40°10' W;
45.– **Águia Branca**, Loc 1 = Sítio Knok, Mata Norte, 18°58' S, 40°44' W; Loc 2 = Fazenda Pedra Redonda, 18°58' S, 40°45' W;
46.– **Ibiritama**, Parque Nacional do Caparaó, 20°25' S, 41°47' W;
47.– **Santa Teresa**, Floresta da Capela São Braz, 19°55' S, 40°59' W;
48.– **Venda Nova**, Hotel Fazenda Monte Verde, 24 km SE de Venda Nova, 20°19' S, 40°59' W;
49.– **Cariacica**, 20°22' S, 40°22' W.

GOIÁS

- 50.– **Anápolis**, [1000 m], 16°20' S, 48°58' W;
51.– **Crixás**, 14°27' S, 49°58' W;
52.– **Formosa**, Rio Canabrava, [162 km N of Brasília], approx. 15°5' S, 47°5' W;
53.– Barra do Rio São Domingos, 13°36' S, 46°48' W;
54.– **Nova Roma**, Cana Brava, 13°51' S, 46°56' W;
55.– **Ipameri**, 17°42' S, 48°8' W;
56.– **Caldas Novas**, 18°0' S, 48°30' W;
57.– **Minaçu**, Usina Hidrelétrica Serra da Mesa, 13°50' S, 48°18' W;
58.– **Colinas do Sul**, 20 km NW Colinas do Sul, 14°9' S, 48°4' W;
59.– **Uruaçu**, 40 km NE Uruaçu, 14°26' S, 48°54' W;
60.– **Niquelândia**, 55 km N of Niquelândia, Usina Hidrelétrica Serra da Mesa, 13°58' S; 48°28' W.

MARANHÃO

- 61.– **Turiação**, Alto da Alegria, [approx. 40 km SW of] Turiação ("Tury-assu", "Jury-assu"), 1°41' S, 45°21' W.

MATO GROSSO

- 62.– **Aripuanã**, 10°9' S, 59°13' W;
63.– **Vila Rica**, 9°54' W, 51°12' W;
64.– **Nova Xavantina**, Loc 1 = Rio das Mortes, [250 m], 14°40' S, 52°21' W;
65.– Serra do Roncador, 264 km N of Xavantina, 12°54' S, 51°52' W;
66.– **Chapada dos Guimarães**, Casa de Pedra, approx. 15°26' S, 55°45' W;
67.– **Barra do Garças**, Fazenda Lagoa Bonita, 36 km N Barra do Garças, 15°34'50" S, 52°22'29" W;
68.– **Ribeirão Cascalheira**, Fazenda Noirumbá, 34 km NW Ribeirão Cascalheira, 12°55' S, 51°37' W.
69.– Capão do Lobo, 16°21' S, 46°54' W.

MATO GROSSO DO SUL

- 70.– **Maracaju**, 500 m, approx. 21°38' S, 55°9' W;
71.– **Ponta Porã**, Fazenda Maringá, 54 km W Dourados, 22°16'47" S, 55°18'36" W, [427 m].

MINAS GERAIS

- 72.– **Indianópolis**, Usina Hidrelétrica Miranda, 18°54'44" S, 48°2'29" W;
73.– **Pedrinópolis**, Mata dos Adolfo, 19°7'20" S, 47°33'45" W, [850 m];
74.– **Pardizes**, Mata de Galeria João Alonso, 19°21'10" S, 47°17'34" W;
75.– **São Roque de Minas**, Loc 1 = Serra da Canastra, 20°13'58" S, 46°22'11" W; Loc 2 = Parque Nacional Serra da Canastra (includes: Loc 1 = 19–25 km W of São Roque de Minas; Loc 3 = Fazenda Barreiro, 1 km N of park; Loc 4 = Casca d'Anta; Loc 5 = Fazenda das Pedras; Loc 6 = Fazenda dos Quartéis; Loc 7 = Retiro Maria do Carmo; Loc 8 = Zezim Cândido), 20°15' S, 46°40' W;
76.– **Piumhi**, Fazenda Varjão, 20°31' S, 45°56' W;
77.– Riacho da Cruz, Rio São Francisco, 15°20' S, 44°14' W;
78.– **Barro Alto**, Rio São Francisco, 15°28' S, 44°24' W;
79.– **Lassance**, Fazenda São Francisco, 17°53'12" S, 44°34'39" W;
80.– **Viçosa**, Mata do Paraíso, 20°45' S, 42°51' W.
81.– **Nova Ponte**, Loc 1 = Mata do Edésio, 8 km NW Nova Ponte, 19°7'50" S, 47°44'22" W [854 m]; Loc 2 = Mata do Vasco, 12 km W Nova Ponte, 19°10'15" S, 47°42'29" W, 878 m; Loc 3 = Usina Hidrelétrica Nova Ponte, 19°7' S, 47°41' W;
82.– **Brumadinho**, Área de Proteção Especial do Rio Manso, 20°8'36" S, 44°11'59" W;
83.– **Belo Horizonte**, Loc 1 = 19°55' S, 46°56' W; Loc 2 = Mata Barreiro, 19°55' S, 43°56' W;
84.– **Santana do Riacho**, Distrito Cardeal Mota, 19°19'54" S, 43°37'24" W;
85.– **Diamantina**, Loc 1 = Mineração Tejuicana, 18°14' S, 43°36' W; Loc 2 = Conselho Mata, 18°14' S, 43°54' W;
86.– **Lagoa Santa**, Rio das Velhas, 19°38' S, 43°53' W;
87.– **Mariana**, 20°23' S, 43°25' W;

- 88.– **Mariléria**, Loc 1 = Parque Estadual do Rio Doce, 19°43' S, 42°39' W; Loc 2 = Parque Florestal do Rio Doce, Rio Turvo, 19°42' S, 42°30' W; Loc 3 = Parque Florestal do Rio Doce, Hotel, 19°46' S, 42°37' W;
- 89.– **São Gonçalo do Rio Preto**, Parque Estadual do Rio Preto, 15 Km S de São Gonçalo, 18°9' S, 43°23' W;
- 90.– **Turmalina**, Estação Ecológica de Acauã, 17 km N de Turmalina, 47°8' S, 42°46' W;
- 91.– **Jequitinhonha**, Torre da TELEMIG, JEQUI C, e XCI, 16°21' S, 41°5' W;
- 92.– **Virgem da Lapa**, Fazenda Paiol, Floresta Alta, Torre da Telemig Jequi XLIII, 16°50'0" S, 42°13'0" W;
- 93.– **Coqueiral**, Área de Proteção Permanente do município de Coqueiral, 21°9'30" S, 45°26'16" W.
- 94.– **Santa Bárbara**, Loc 1 = Parque Natural do Santuário do Caraça, 25 km SW Santa Bárbara, 20°5'0" S, 43°30'0" W, 1300 m; Loc 2 = Catas Altas: Reserva Peti, 19°53'31" S, 43°22'6" W;
- 95.– **Fervedouro**, Parque Estadual da Serra do Brigadeiro, Fazenda Neblina, 20 km W Fervedouro, 20°43' S, 42°29' W, 1300 m;
- 96.– **Lima Duarte**, Parque Estadual do Ibitipóca, 21°33' S, 43°55' W;
- 97.– **Bocaiúva**, Distrito Carne Seca, 17°23'20" S, 45°53'43" W;
- 98.– **Coronel Murta**, Ponte do Colatino, 16°36' S, 42°12' W;
- 99.– **Jaíba**, Parque Florestal do Jaíba, 15°5' S, 43°47' W;
- 100.– **Manga**, Mocambinho, 14°55' S, 43°55' W;
- 101.– **Palmítal**, 16°36' S, 41°47' W;
- 102.– **Formoso**, Parque Nacional Grandes Sertões Veredas, 14°56' S, 46°14' W;
- 103.– **Salinas**, 16°10' S, 42°17' W;
- 104.– **Passos**, 20°43' S, 46°37' W;
- 105.– **Poços de Caldas**, 21°48' S, 46°34' W;
- 106.– Serra do Cipó, 1400 m, 19°25' S, 43°35' W;
- 107.– Engenho Velho, highway BR-262 km 53, 20°15' S, 42°12' W;
- 108.– **Caratinga**, Estação Biológica de Caratinga, Fazenda Montes Claros, 19°50' S, 41°50' W

PARÁ

- 109.– **Belém**, Bosque Municipal; Utinga; Bussuquiara, 1°27' S, 48°29' W;
- 110.– Rio Moju, 1°40' S, 48°25' W;
- 111.– Estrada Belém-Brasília, km 94, 1°19' S, 47°42' W;
- 112.– São Domingos do Capim ("Capim"), Estrada BR14 km 87, 1°41' S, 47°47' W;
- 113.– Serra dos Carajás, área N1, Casa de Pedra, approx. 6°0' S, 51°30' W;
- 114.– **Parauapebas**, Fazenda São Luiz, 6°16' S, 50°39' W;
- 115.– **Altamira**, Loc 1 = East bank Rio Xingu, 52 km SSW Altamira, 3°38' S, 52°22' W; Loc 2 = Cachoeira Espelho, 52 km SSW Altamira, E bank Rio Xingu, 3°39' S, 52°22' W;
- 116.– Caxiuanã, 1°36' S, 51°37' W;
- 117.– Posto Monte Dourado, 105 km S and 170 km W of Macapá, W of Rio Jari, 0°50' S, 52°33' W;
- 118.– **Oriximiná**, Porto Trombetas, Rio Saracazinho km 43, 1°42' S, 56°23' W;
- 119.– **Aramanai** ("Aramanay"), Rio Tapajós, 2°45' S, 54°59' W;
- 120.– Igarapé Maróí ("Marai"), E bank Rio Tapajós, 2°51' S, 55°3' W;
- 121.– Curuá-Una, 44 km S and 40 km E of Santarém, 2°50' S, 54°22' W;
- 122.– Tauari ("Tauary"), E bank Rio Tapajós, 3°5' S, 55°6' W;
- 123.– **Aveiro** ("Aveiros"), E bank Rio Tapajós, 3°15' S, 55°10' W;
- 124.– **Itaituba**, Parque Nacional da Amazônia, approx. 4°30' S, 56°15' W;
- 125.– **Santarém**, Boim, W bank Rio Tapajós, 2°49' S, 55°10' W;
- 126.– Igarapé Amorim ("Amorim"), Rio Tapajós, 2°26' S, 55°0' W.

PARAÍBA

- 127.– **Areia**, Reserva Estadual Mata do Pau-Ferro, 6°57' S, 35°44' W;
- 128.– **Rio Tinto**, Reserva Biológica Guaribas, SEMA III, 6°48' S, 35°5' W.

PERNAMBUCO

- 129.– **Caruaru**, Loc 1 = Parque Municipal Vasconcelos Sobrinho, Serra dos Cavalos, 13 km ESE de São Caitano 8°17'42" S, 35°58'22" W; Loc 2 = Sítio Brejo do Buraco, 8°17' S, 35°58' W; Loc 3 = Sítio Quandus, 8°17' S, 35°58' W; Loc 4 = Sítio Serra dos Cavalos, 8°21' S, 36°2' W; Loc 5 = Fazenda Santa Maria, 8°23' S, 36°2' W [850 m], Loc 6 = Fazenda Caruaru, 8°22' S, 36°3' W;
- 130.– **Brejo da Madre de Deus**, Sítio Rita, Mata Buriti, 8°9' S, 36°22' W;
- 131.– **Garanhuns**, Sítio Cavaquinho, 8°54' S, 36°29' W;
- 132.– **Bonito**, 8°35' S; 35°47' W;
- 133.– **Jaqueira**, Loc 1 = RPPN Frei Caneca, 8°42' S, 35°50' W, includes Mata do Cruzeiro; Loc 2 = Mata do Fervedouro; Loc 3 = Mata do Ajeró;
- 134.– **Inajá**, Reserva Biológica Serra Negra, 8°38' S, 38°1' W;
- 135.– **Cabo de Santo Agostinho**, Reserva Ecológica do Gurjáú, Mata do Café, 8°15' S, 35°5' W;
- 136.– **Exu**, Sítio Mangueira, 8.5 km NE de Exu, 7°28'47" S, 39°39'5" W;
- 137.– **Bezerros**, Vertentes, 8°11'31" S, 35°47'35" W;

PIAÚ

- 138.– **Caracol**, Parque Nacional Serra das Confusões, 9°13' S, 43°27' W;
- 139.– **Guadalupe**, 6°50' S; 43°30' W

RIO DE JANEIRO

- 140.– **Teresópolis**, Fazenda Guinle [= Fazenda Comari], 22°27' S, 42°57' W;
- 141.– **Itatiaia**, Parque Nacional do Itatiaia, 22°26'24" S, 44°37'12" W;
- 142.– **Mangaratiba**, Ilha da Marambaia, 23°3' S, 43°58'12" W;
- 143.– **Casimiro de Abreu**, Fazenda União, 20 m, 22°45' S, 42°2' W;
- 144.– **Angra dos Reis**, Loc 1 = Vila Dois Rios, Ilha Grande, 23°9' S, 44°14' W; Loc 2 = Praia Vermelha, Ilha Grande, 23°9' S, 44°21' W, Loc 3 = 1.1 km SW Abraão, Ilha Grande, approx. 23°8'57.7" S, 44°10'37.7" W;
- 145.– **Paraty**, Tarituba, 23°1'48" S, 44°34'48" W;
- 146.– **Guapimirim**, Loc 1 = Garrafão, 22°39' S, 43°2' W; Loc 2 = Fazendas Consorciadas, 22°34'48" S, 42°54'36" W; Loc 3 = Centro de Primatologia da FEEMA, 22°37'48" S, 42°58'12" W

RONDÔNIA

- 147.– Usina Hidrelétrica de Samuel, Rio Jamari, 8°45' S, 63°28' W

RORAIMA

- 148.– **Maracá**, Ilha de Maracá, 3°22' N, 61°26' W;
- 149.– **Pacaraima**, Limão, Rio Cotinha, 3°56' N, 60°30' W;
- 150.– Fazenda Deus-me-ajude, 4°16' N, 61°2' W;

SÃO PAULO

- 151.– **Casa Grande**, 23°48' S, 45°25' W;
- 152.– **Pilar do Sul**, 23°49' S, 47°41' W;
- 153.– **Salesópolis**, Estação Biológica de Boracéia, 3 km E, 28 km SE Biritiba, 23°39' S, 45°54' W;
- 154.– **São Sebastião**, 23°48' S, 45°25' W.
- 155.– Porto do Rio Paraná, 19°59' S, 47°46' W;
- 156.– **São José do Rio Preto**, 20°48' S, 49°23' W;

TOCANTINS

- 157.– **Peixe**, Rio Santa Teresa, 20 km NW from Peixe, 11°50'34" S, 48°38'8" W;
- 158.– **Lagoa da Confusão**, Fazenda Lago Verde, 10°52'9.1" S, 49°41'52.1" W;
- 159.– **Pium**, 10°27' S, 49°38' W;
- 160.– **Jalapão**, 10°22' S, 47°25' W;
- 161.– **Paraná**, 12°33' S, 47°45' W.